Hindawi
Geofluids
Volume 2023, Article ID 1750844, 23 pages
https://doi.org/10.1155/2023/1750844

Research Article

Dynamic Response Analysis of Roadway Surrounding Rock Induced by Dynamic Load under the Action of Hard and Thick Rock Stratum

Kaihua Liang,[1,2] Quansen Wu,[3] Quanlin Wu,[3,4] Xiang Shi,[1,2] Hong Zhao,[1,5,6] Fuwu Ma,[1,2] and Zhaomin Zhang[1,2]

[1]*Engineering Laboratory of Deep Mine Rockburst Disaster Assessment, Shandong Province, Jinan 250100, China*
[2]*Shandong Province Research Institute of Coal Geology Planning and Exploration, Jinan 250100, China*
[3]*Jining University, Qufu 273100, China*
[4]*Yankuang Energy Group Company Limited, Zoucheng 273500, China*
[5]*Physical Exploration and Survey Team of Shandong Bureau of Coal Geology, Jinan 250100, China*
[6]*Shandong Taishan Resources Prospecting Group Ltd., Taian 271000, China*

Correspondence should be addressed to Quansen Wu; 2401392747@qq.com and Quanlin Wu; jnxywql@163.com

Received 24 March 2022; Revised 22 June 2022; Accepted 13 July 2022; Published 30 April 2023

Academic Editor: Yong-Zheng Wu

Copyright © 2023 Kaihua Liang et al. This is an open access article distributed under the Creative Commons Attribution License, which permits unrestricted use, distribution, and reproduction in any medium, provided the original work is properly cited.

In the process of coal seam mining, there are often hard thick key layers in the overlying strata. Due to the high strength and good integrity of the hard thick key layer, after the hard thick key layer is broken, the overlying strata will collapse and lose stability in a large area, which is very easy to induce dynamic disasters such as rock burst, mine earthquake, coal wall caving, and roof slab caving. Aiming at the hard and thick key layer overlying the working face, the dynamic response of the mine under the strong mine earthquake induced by the breaking of the main key layer of high-level magmatic rock is numerically simulated and analyzed by using FLAC2D numerical simulation software, and the variation laws of the stress field, displacement field, and velocity field of the coal seam roadway under different boundary conditions and different focal heights are studied. The research shows that the roof of solid coal roadway is prone to vibration in a small range, and the displacement increases and decreases with the disturbance. The displacement of the floor and two sides of the solid coal roadway and the top floor and two sides of the roadway along the goaf continues to increase in the initial stage of the disturbance, and the displacement will remain stable with the continuation of the disturbance. The displacement of both sides and roof and floor of gob roadway can reach stability in the later stage of disturbance, and with the increase of the number of adjacent goaf, the longer it takes for the displacement of surrounding rock to reach stability. When the focal height is lower than 90 m, the variation of surrounding rock response increases sharply with the decrease of focal height. When a strong earthquake occurs in the low rock stratum, the impact damage of roadway surrounding rock is almost inevitable. The influence degree of strong earthquake on the stability of roadway surrounding rock is arranged as follows: gob-side roadway (mined out on one side) > solid coal roadway (mined out on both sides) > solid coal roadway (mined out on one side). The evolution process also shows that the working face boundary conditions have an important influence on the energy propagation of mine earthquake. With the increase of the number of adjacent goafs, the faster the energy attenuation rate of mine earthquake propagation is. The research results have important reference significance for the safe mining of working face under similar geological conditions.

1. Introduction

With the continuous increase of mining depth and in-situ stress, mine dynamic phenomena or disasters such as mine earthquake, rock burst, coal and gas outburst, and support dynamic load are becoming more and more serious [1–6]. Relevant studies show that the range of overburden movement and stress field related to dynamic disasters in deep

mining has exceeded the range of traditional basic roof in the longitudinal direction. In particular, when the overburden of the working face has a hard and thick key layer, due to the good integrity of the hard and thick key layer and the large first breaking span, under the bearing and shielding effect of the hard and thick key layer, the abutment pressure concentration of the working face before the breaking of the super thick key layer is high and the separation space under the key layer is large. When the suspension span length of the hard thick key layer reaches the limit suspension span length, the key layer will break [7–9]. Due to a large amount of separation space under the hard thick key layer, the broken magmatic rock block sinks rapidly, generates intense instantaneous kinetic energy, releases a large amount of energy, and produces mine earthquakes. When the energy is large enough, there are even produce strong earthquakes [10, 11]. The combined action of mine earthquake and highly concentrated static load of working face is easy to cause coal wall caving and roof caving and even induce rockburst. Hard and thick key layers are distributed in most mining areas in China, such as Huaibei coalfield, Yanzhou coalfield, and Datong coalfield [12–14]. For example, the 400–800 m thick conglomerate overlying Huafeng coal mine has abnormal abutment pressure and rock burst from time to time. Since 1992, the impact has occurred tens of thousands of times rock burst, and the maximum magnitude is as high as 2.9. The number of rock burst that caused damage to the working face reached 108 times, forcing the working face to stop production for 12 times, resulting in 43 serious injuries and many deaths, and resulting in countless times of roadway maintenance, which had an adverse impact on social and economic benefits. There is 94.27 m thick medium sandstone in the upper 91 m of the third coal layer in the second mining area of Baodian coal mine. The extremely thick medium sandstone is cut by Machang fault outside the stopping line of 2310, 2311, and 2312 working faces. After the 2310, 2311, and 2312 working faces are mined out, the huge thick medium sandstone cut is suspended in a large area and is in a dynamic equilibrium state, and the huge thick medium sandstone is prone to large-area movement. On September 6, 2004, a rock burst accident occurred in no. 1 air inlet connection lane of 2310 working face of Baodian coal mine, and the seal was broken, resulting in two deaths and six injuries. According to the analysis, the accident was caused by the mining earthquake caused by the large-area movement of the huge thick medium sandstone on the upper part of the goaf. The shock wave generated by the mining earthquake destroyed the closed wall, and the impact spread to the thrown closed bricks, resulting in casualties. The rockburst is serious under the condition of high-level huge thick conglomerate in Huafeng coal mine and Qianqiu Coal Mine. The rock burst and coal and gas outburst in Haizi coal mine and Yangliu Coal Mine are related to the fracture of high-level magmatic rock overburden. Through the above dynamic disaster analysis, it can be seen that when the working face is covered with hard thick rock stratum, the dynamic disaster caused by the breaking of hard thick rock stratum seriously threatens the safe and efficient production of coal mine. Therefore, people must pay great attention to the dynamic disaster caused by the breaking of hard and thick rock strata in the mining process of the working face.

At present, many well-known scholars have done a lot of research on the occurrence mechanism of mining dynamic disasters under hard and thick key layers, the change characteristics of overburden structure, and the characteristics of stress evolution by using the methods of theoretical analysis, numerical simulation, and field observation [13, 15–20]. He [21] and others adopted the key layer theory of rock movement and obtained through analysis that the mine pressure reaches the maximum when the key layer of overburden is broken, which is very easy to lead to strong mine earthquake and rockburst. Jiang [10] and others used the method of theoretical analysis to deduce the fracture calculation method of hard and thick key layers and verified the calculation method through field dynamic response observation. Hu [22] and others established a numerical model of mining under similar geological conditions by using FLAC3D numerical simulation and simulated and analyzed the causes of dynamic load disasters induced by hard and thick strata. Jiang et al. used FLAC3D numerical simulation calculation method to study the movement law, mining stress evolution characteristics, energy distribution characteristics of overlying strata under hard thick igneous rocks, and the influence of igneous rock occurrence horizon and thickness on the movement law, stress distribution, and energy distribution of overlying strata [23]. Wu et al. took the 103 upper 02 working face of Baodian coal mine as an engineering example, studied the breaking law of overlying hard thick sandstone caused by working face mining according to the field measured microseismic data, and explained the relationship between microseismic data and rock movement [24]. Ning et al. carried out microseismic monitoring on the existing hard and thick rock strata covered on the working face, studied the relationship between the fracture of hard and thick rock strata and microseismic data by using the microseismic distribution law, and put forward prevention and control measures [25]. Yang et al. comprehensively used similar material test, theoretical analysis, and numerical simulation methods to study the deformation and failure of overlying super thick key layer and the variation characteristics of working face bearing pressure and analyzed the mechanism and manifestation mode of working face rock burst induced by the failure of super thick key layer [26]. To sum up, the existing research results play an important role in the prediction and prevention of mining dynamic disasters under hard and thick strata, but they mostly stay in the stage of static load, ignoring the dynamic load effect in the process of coal mining after hard and thick strata are broken.

Based on this, aiming at the occurrence of hard and thick igneous rocks overlying the working face, this paper uses FLAC2D numerical simulation software, numerically simulate and analyze the dynamic response of the mine under the strong mine earthquake induced by the breaking of the main key layer of high-level magmatic rock, and study the variation laws of the stress field, displacement field, and velocity field of the coal seam roadway under different boundary conditions and different focal height. The second part is the description of numerical model. The third part studies the influence law of boundary conditions on roadway

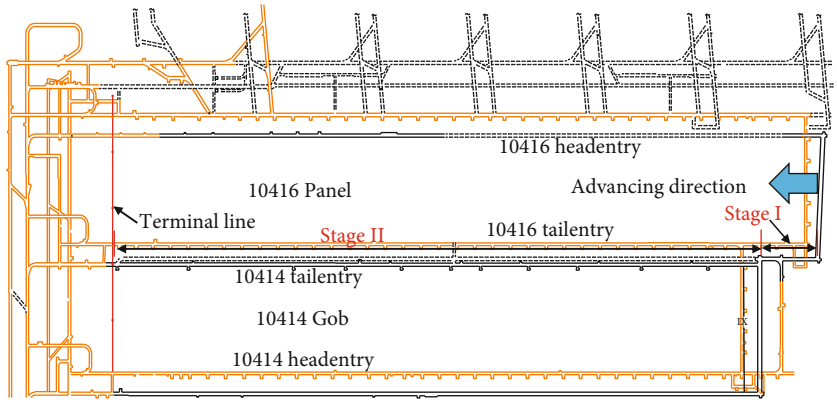

Figure 1: The plane layout of the working face.

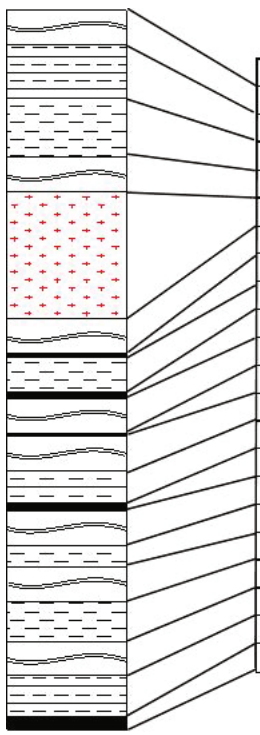

Rock thickness (m)	Depth (m)	Lithology
12.62	394.04	
15.43	409.46	Mudstone
17.13	426.59	Siltstone
14.88	441.47	
43.60	485.07	Igneous rock
2.81	487.88	
1.16	489.04	Coal seam #7_1
7.62	496.66	Siltstone
1.6	499.38	Coal seam #7_2
1.89	501.27	
0.82	502.09	Coal seam #8_1
3.07	505.15	
9.26	514.41	Sandstone
2.23	516.64	Coal seam #8_2
2.25	518.89	
6.30	525.19	Siltstone
28.57	553.76	
11.45	565.76	Siltstone
10.09	575.30	
11.60	589.90	Mudstone
3.54	590.90	Coal seam #1_0

Figure 2: The borehole histogram.

dynamic response. The fourth part is the influence of focal height on roadway dynamic response. The fifth part verifies the correctness of the research through the field data measurement. The research results of this paper have important guiding significance for safe and efficient mining of working face under similar geological conditions.

2. Model Description

2.1. General Engineering Geology Conditions. Taking the geological conditions of 10416 working face in Yangliu Coal Mine as the engineering background, a numerical calculation model is established. The northeast of the working face is the solid coal of mining area 106, and the southwest is the goaf of working face 10414. A 5 m section of protective coal pillar is reserved. The inclined length of the working face is 180 m, the average thickness of the coal seam is 3.5 m, the average inclined angle is 4°, and the buried depth is -570–-610 m. There are two layers of magmatic rocks in the upper part of 10416 working face, which intrude along the roof of 5_2 coal seam and 7_2 coal seam, respectively. The average thickness of the magmatic rock in the roof of coal seam 5_2 is 31.5 m, the average thickness of the magmatic rock in the roof of coal seam 7_2 is 43.5 m, and the average distance between the magmatic rock in the roof of coal seam 5_2 and the magmatic rock in the roof of coal seam 7_2 is 116 m. The plane layout of the working face is shown in Figure 1, and the borehole histogram is shown in Figure 2 [11].

2.2. Establishment of Numerical Model. In this paper, two numerical calculation models are established. The model size, rock composition, and mechanical parameters are the same. When simulating the mining of working face, the mechanical boundary conditions of working face are different.

Table 1: Mechanical parameters and strata of model.

Lithology	Density/kg•m^{-3}	Bulk modulus/GPa	Shear modulus/GPa	Cohesion/MPa	Tensile strength/MPa	Friction angle/°
Coal	1350	4.8	3.6	1	0.8	28
Sandstone	2530	26.4	20.7	4.3	3.8	37
Magmatic rock	3000	38.7	29.7	6.2	7.5	42
Fine sandstone	2530	12.3	8.3	3.4	3.2	35
Siltstone	2530	15.2	9.4	2.8	2.4	30
Mudstone	2340	7.1	5.1	1.2	2.4	25

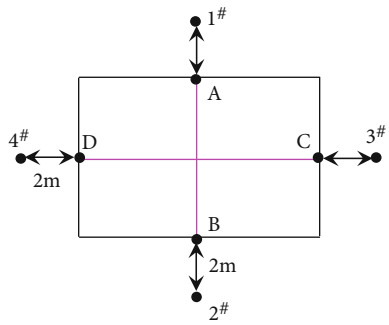

Figure 3: Layout of monitoring points.

The first model is the mining of solid coal face on both sides. The second model is the working face mining with one side of solid coal and one side of goaf. According to the research content of this paper, two identical numerical models are established, and the model size is 660 m (length) × 208 m (height), roadway size 5 m (width) × 3 m (high), the buried depth of the simulated coal seam is 600 m, and the vertically uniformly distributed load of 10.75 MPa is applied on the top of the model. The composition and mechanical parameters of model rock stratum can be seen in Table 1.

The calculation process of the two numerical models is divided into 5 steps. Step 1: establish the model and initialize the stress field. Step 2: excavate two roadways in the working face (model 1), and excavate one side of the working face into a goaf (model 2). Step 3: static field balance. Step 4: the displacement and velocity of static field are cleared. Step 5: apply disturbance load and monitor the mechanical response of roadway surrounding rock.

2.3. Numerical Simulation Scheme. Four displacement monitoring points A, B, C, and D are arranged at the midpoint of the roadway top and floor and two sides of the working face (the side of the working face is called the inner side, and the side of the roadway far away from the working face is called the outer side), and 1#, 2#, 3#, and 4# four stress monitoring points are arranged 2 m outside the displacement monitoring points (as shown in Figure 3) to monitor the stress field, displacement field, and the variation law of velocity field and acceleration field.

(1) During the mining process of the working face, strong earthquake events have occurred at the bottom of magmatic rock for many times. In view of this, apply strong disturbance at the bottom of magmatic rock in models 1 and 2 (116 m away from the coal seam) and monitor the dynamic response law of roadway surrounding rock

(2) For models 1 and 2, apply strong disturbances are at 50 m, 70 m, and 90 m above the coal seam to analyze the dynamic response law of roadway surrounding rock under different focal heights

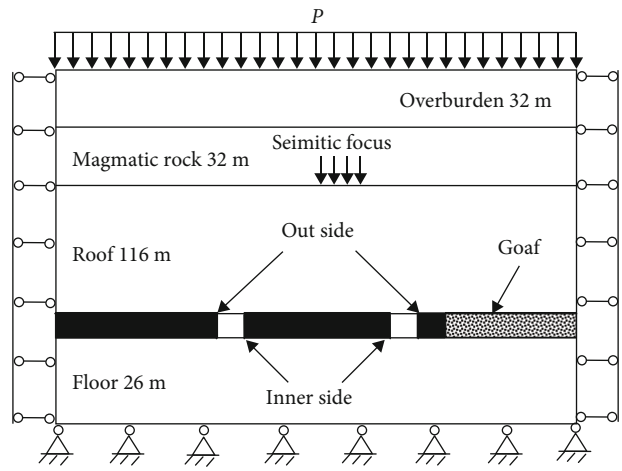

Figure 4: Numerical calculation model.

The strong earthquake distance M_0 above the working face is 1.0×10^{13} N · m, converted into Richter scale $M_L = 2.56$ and vibration energy $E = 4.55 \times 10^6$ J, dominant frequency $f_0 = 50$ Hz. The dynamic calculation time is set to 1.0 s, and the static boundary setting and Rayleigh damping are adopted. The model adopts plane strain analysis, the calculation and analysis criterion adopts Mohr Coulomb strength criterion, and the goaf and working face roadway are simulated by empty element. The schematic diagram of the model (taking model 2 as an example) is shown in Figure 4.

3. Influence of Boundary Conditions on Dynamic Response of Roadway

3.1. Solid Coal on Both Sides of Working Face

(1) Dynamic response of roadway surrounding rock

Figure 5 reflects the dynamic response characteristics of roadway surrounding rock under the condition that the focal

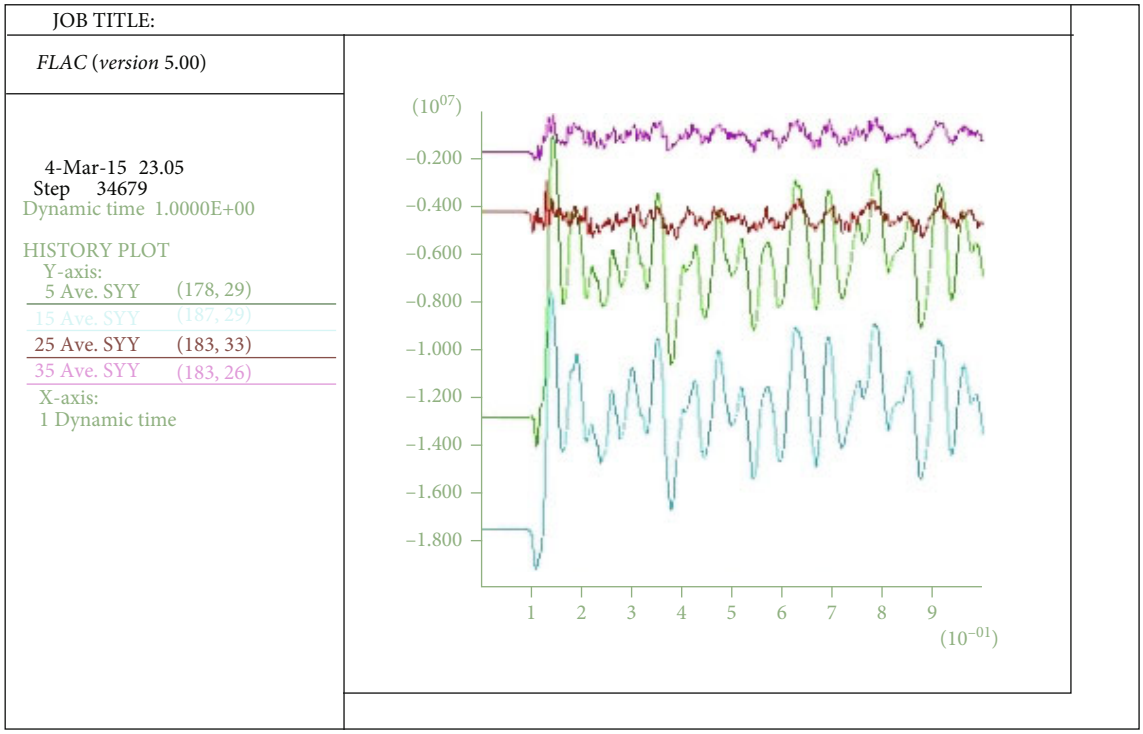

(a) Vertical stress variation of roadway roof, floor, and two sides

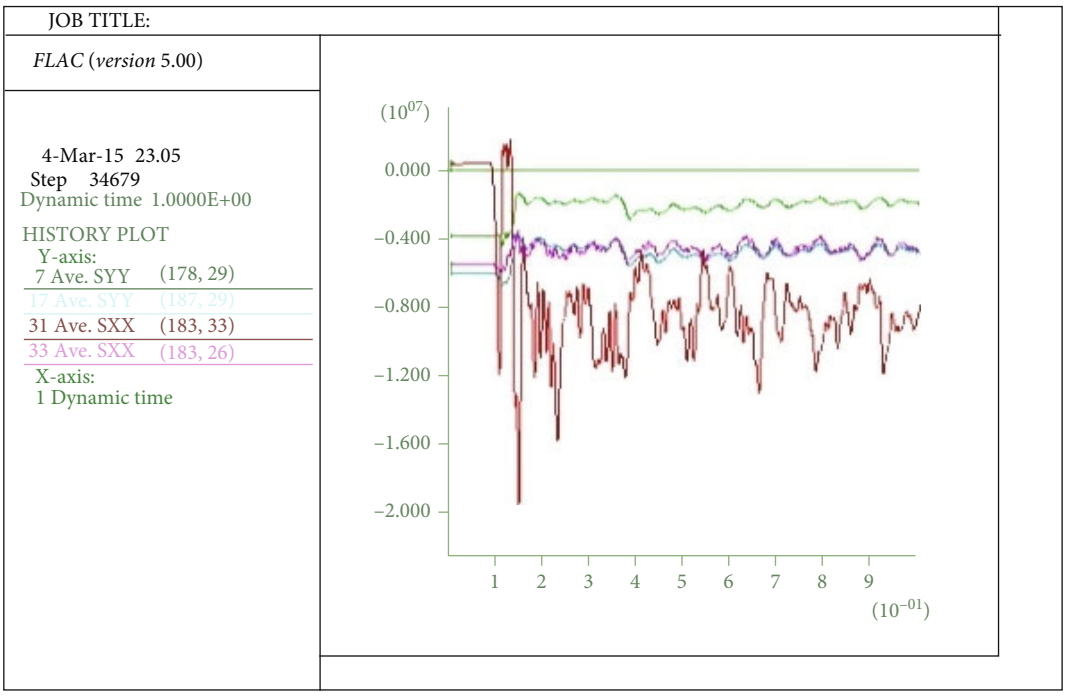

(b) Horizontal stress variation of roadway roof, floor, and two sides

Figure 5: Continued.

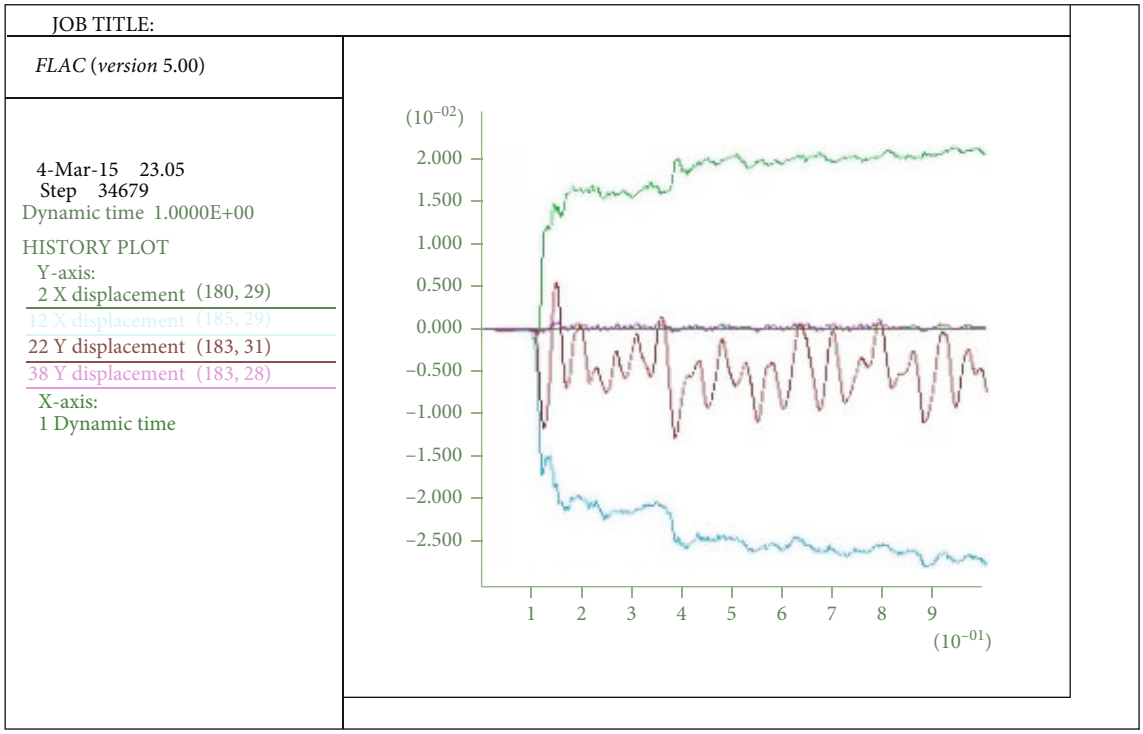

(c) Displacement of roof, floor, and two sides of roadway

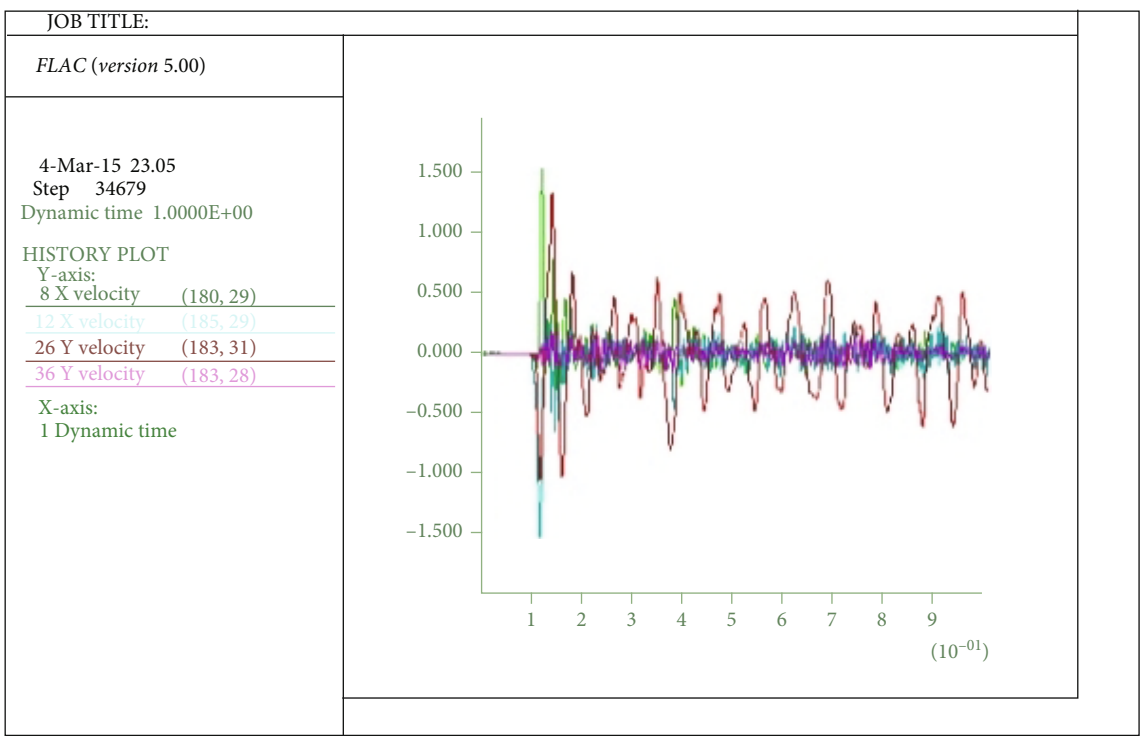

(d) Displacement speed of roadway roof and floor and two sides

Figure 5: Continued.

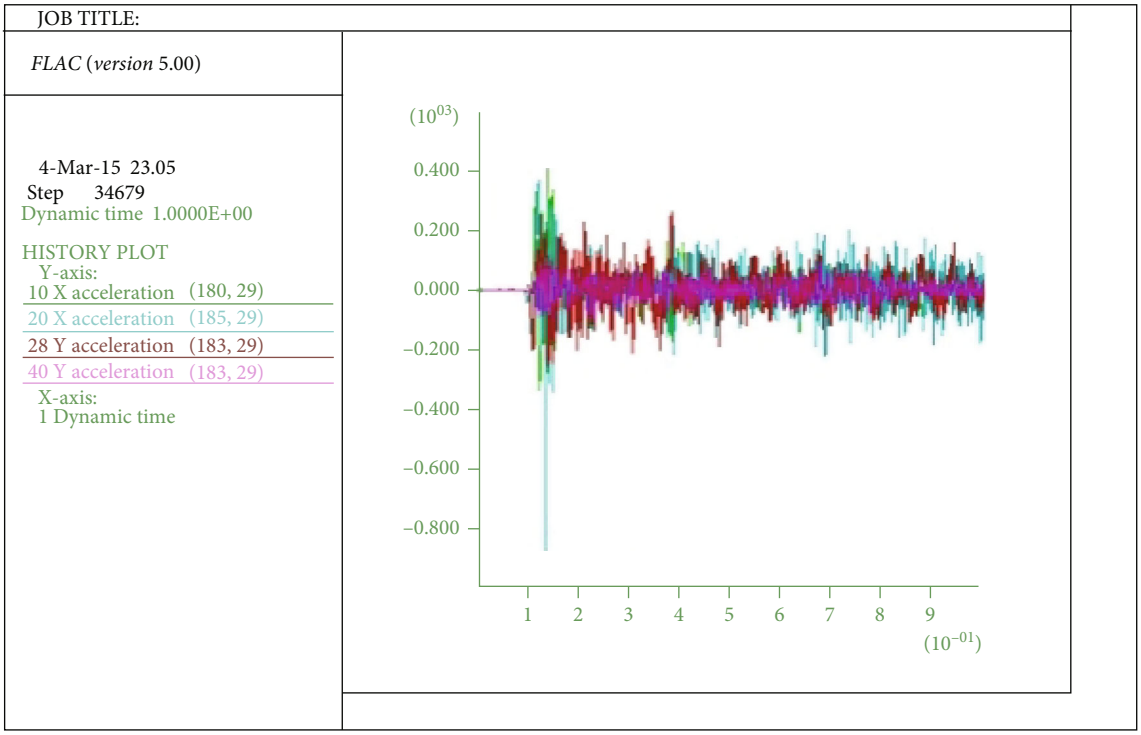

(e) Displacement acceleration of roadway roof and floor and two sides

Figure 5: Dynamic response of roadway surrounding rock under the condition of solid coal on both sides.

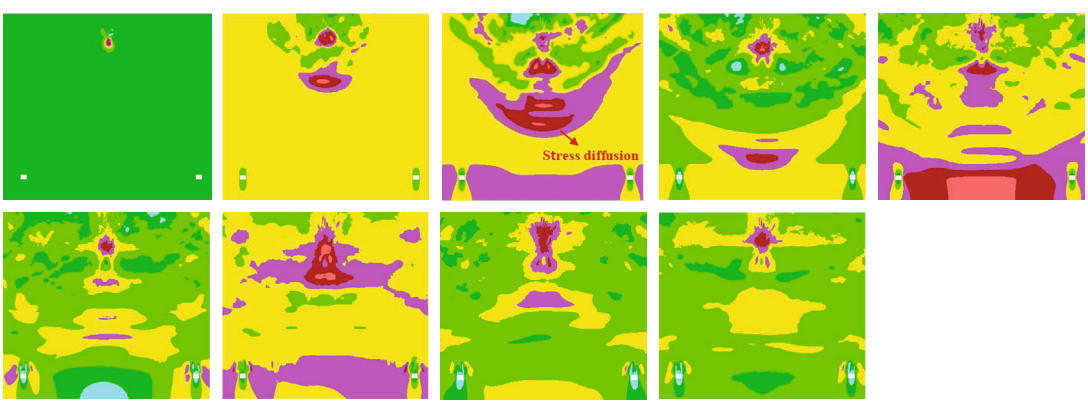

Figure 6: Temporal and spatial evolution law of vertical stress field of roadway surrounding rock under strong earthquake disturbance.

point is located at the bottom of magmatic rock and solid coal on both sides of the working face. It can be seen from Figure 5 that under the influence of strong earthquake, the horizontal stress, vertical stress, and displacement of surrounding rock of roadway have changed, but there are significant differences in change sensitivity.

In terms of stress, the influence of mine earthquake on stress is mainly reflected in the horizontal stress of roof and the vertical stress of inner wall. After 0.11 s disturbance, the vertical stress of the inner wall instantly reaches 19.36 MPa, and the inner wall compresses sharply and then decreases to 8.01 MPa. In the process of sharp increase and decrease of stress, the energy is released rapidly, which is easy to form dynamic phenomena such as rock burst and microseism. After 0.38 s of disturbance, the peak value of vertical stress in the inner wall decreases and fluctuates between 9.3 and 15.4 MPa. The stress change trend of the outer wall is the same as that of the inner wall. The vertical stress of the top and bottom plate is at a low level, and the stress level basically reaches a stable state after 0.15 s disturbance. For the horizontal stress, when the disturbance is 0.15 s, the horizontal stress of the top plate reaches the maximum value of 20.62 MPa. After 0.23 s, the horizontal stress decreases greatly and fluctuates between 4.98 and 13.6 MPa. After 0.36 s, the horizontal stress of the bottom plate and two sides is basically stable.

In terms of displacement, the deformation of both sides of the roadway is greater than that of the roof and floor, and the floor deformation is basically not affected by disturbance. For the upper part, the displacement of the upper part

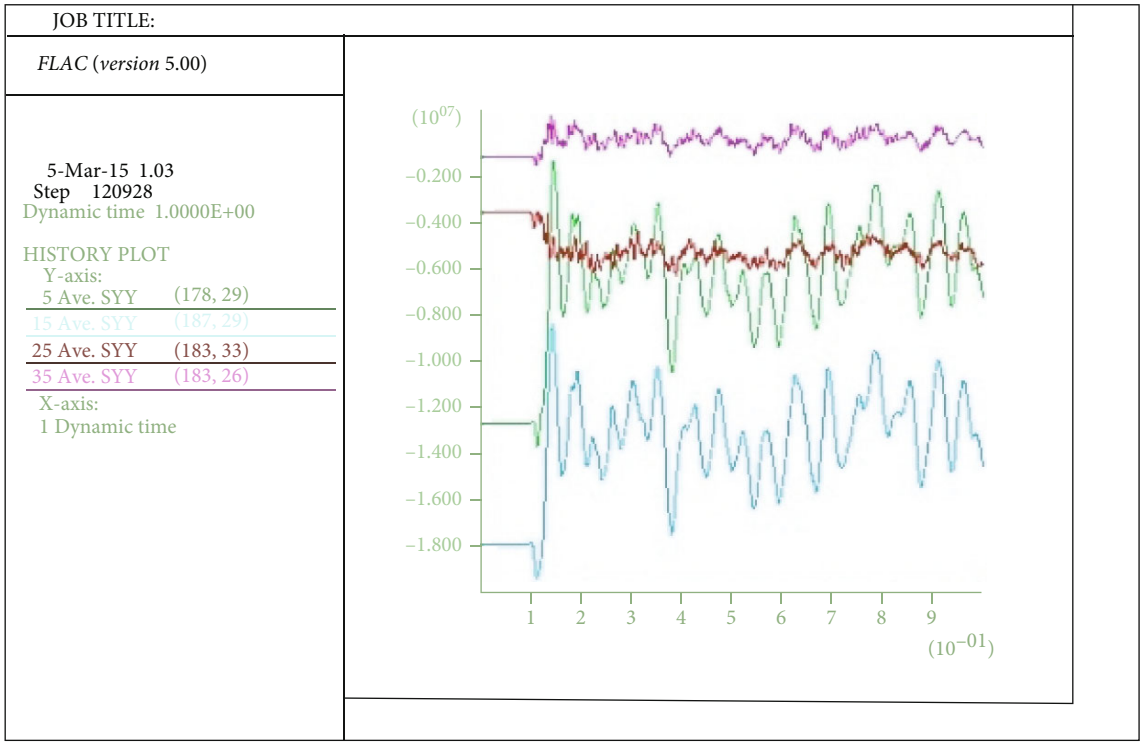

(a) Vertical stress variation of roadway roof, floor, and two sides

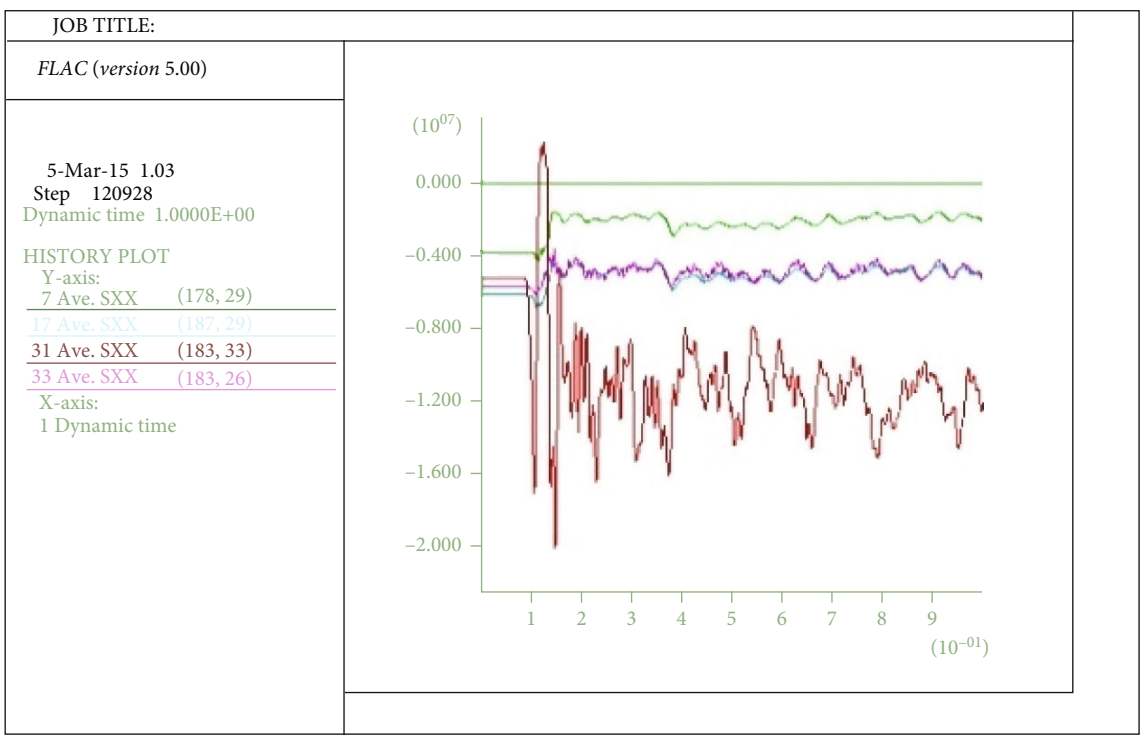

(b) Horizontal stress variation of roadway roof, floor, and two sides

Figure 7: Continued.

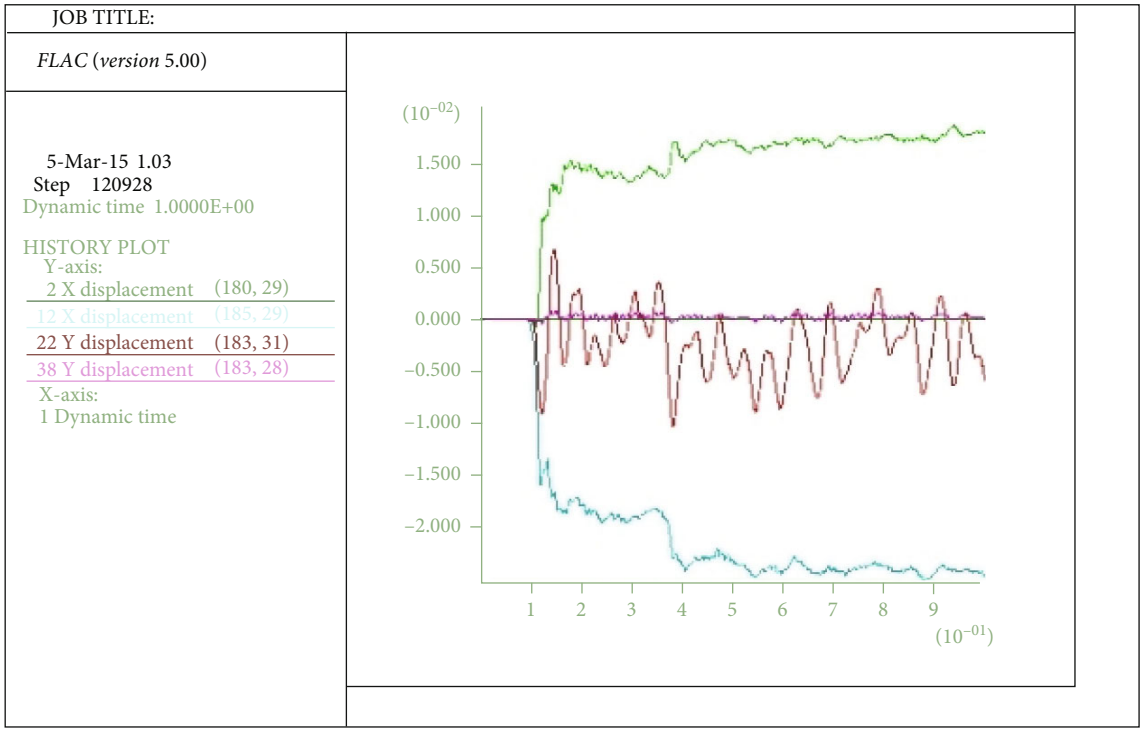

(c) Displacement of roof, floor, and two sides of roadway

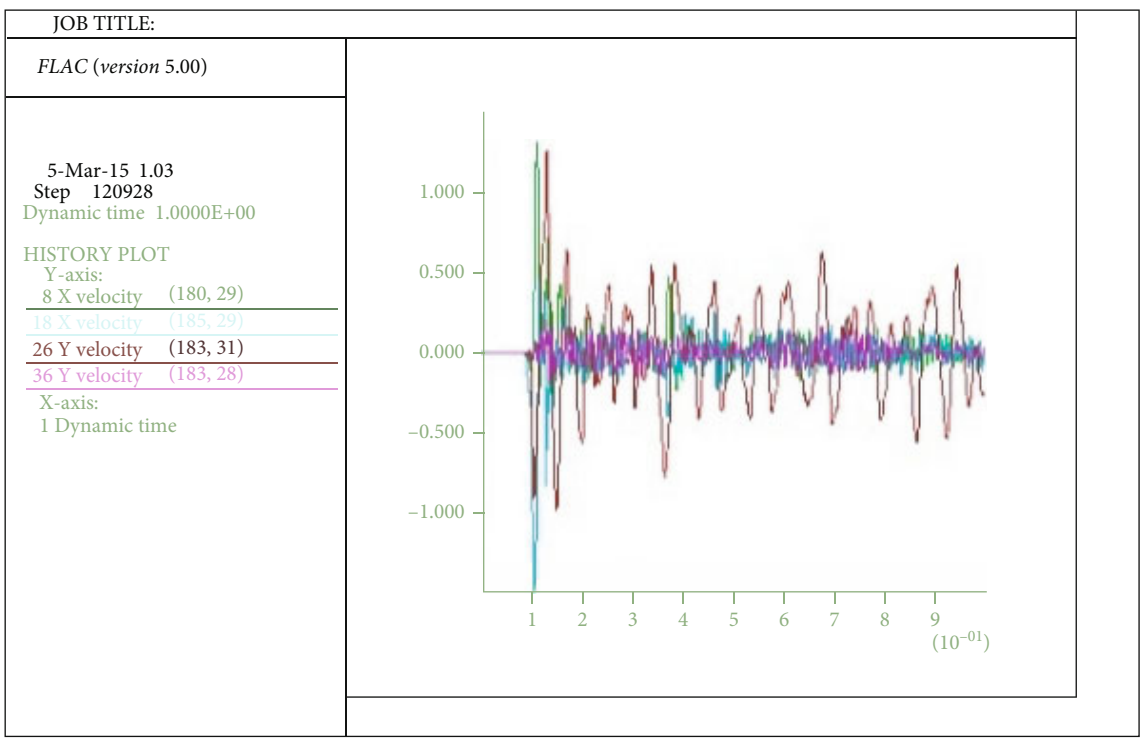

(d) Displacement speed of roadway roof and floor and two sides

Figure 7: Continued.

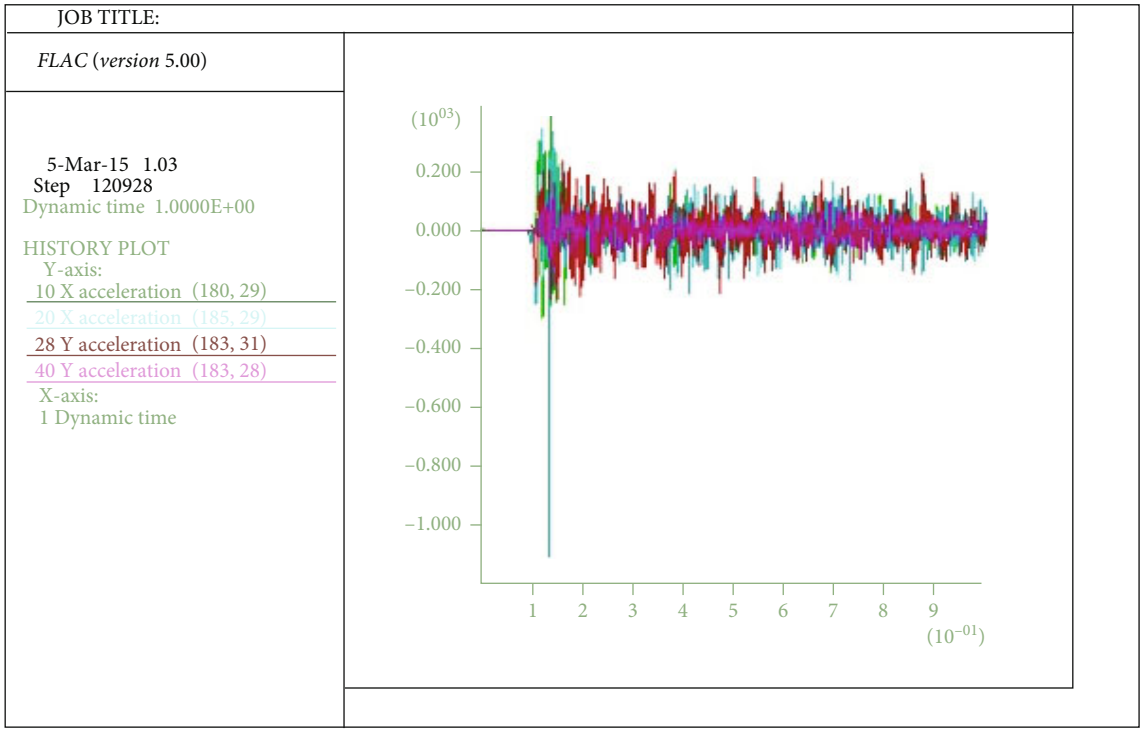

(e) Displacement acceleration of roadway roof and floor and two sides

Figure 7: Dynamic response of surrounding rock in solid coal roadway.

increases linearly during the disturbance of 0–0.11 s. After 0.38 s of disturbance, the displacement is basically stable. Finally, the maximum displacement of the outer side reaches 21.05 mm, and the displacement of the inner side reaches 27.28 mm. For the roof, the displacement fluctuates in a small range, which will cause roof vibration.

In terms of deformation speed, there is little difference between the maximum displacement speed of the two sides of the roadway and the roof, which are 1.53 m/s for the outer side, 1.54 m/s for the inner side, and 1.33 m/s for the roof, respectively, and the maximum displacement speed of the floor is only 0.19 m/s. In terms of deformation acceleration, the displacement acceleration of the two sides is very different, which are 404 mm/s^2 for the outer side and 887.07 mm/s^2 for the inner side. The deformation acceleration of the roof and floor is small, which are 261 m/s^2 for the roof and 94 m/s^2 for the floor.

Generally speaking, under the condition of solid coal on both sides, the damage degree of the two sides of the roadway after strong earthquake disturbance is greater than that of the roof and floor, and the damage degree of the inner side is greater than that of the outer side.

(2) Spatial evolution characteristics of impact failure of roadway caused by strong earthquake

In order to more vividly show the impact damage effect of strong earthquake on roadway surrounding rock, the movie function of FLAC2D software is used to record the evolution characteristics of roadway surrounding rock stress field in detail according to a certain time step, as shown in Figure 6.

It can be seen from Figure 6 that after the strong earthquake disturbance, the stress wave rapidly propagates downward and attenuates in a spherical manner. During the propagation process, the radiation range of the stress wave continues to expand. When $t = 1500$ time steps, it reaches the direct top of the coal seam, and then the inner wall stress of the roadway in the working face increases significantly. As the simulation continues, the roadway will be significantly deformed. By comparing the vertical stress distribution characteristics under different time steps, it can be seen that the stress propagation takes the middle of the working face as the axis of symmetry and presents a symmetrical distribution shape, and the stress level of the inner side of the roadway is higher than that of the outer side.

3.2. One Side Gob Face Working Face

3.2.1. Dynamic Response of Roadway Surrounding Rock. Figures 7 and 8 reflect the dynamic response characteristics of roadway surrounding rock under the condition that the seismic focus is located at the bottom of magmatic rock and the goaf on one side of the working face. It can be seen from Figure 7 that the mechanical response law of surrounding rock of solid coal roadway in working face under the condition of one side goaf is similar to that of solid coal roadway on both sides, with only slight differences in value and stability time. When the disturbance is 0.15 s, the horizontal stress of the roof reaches the maximum value of

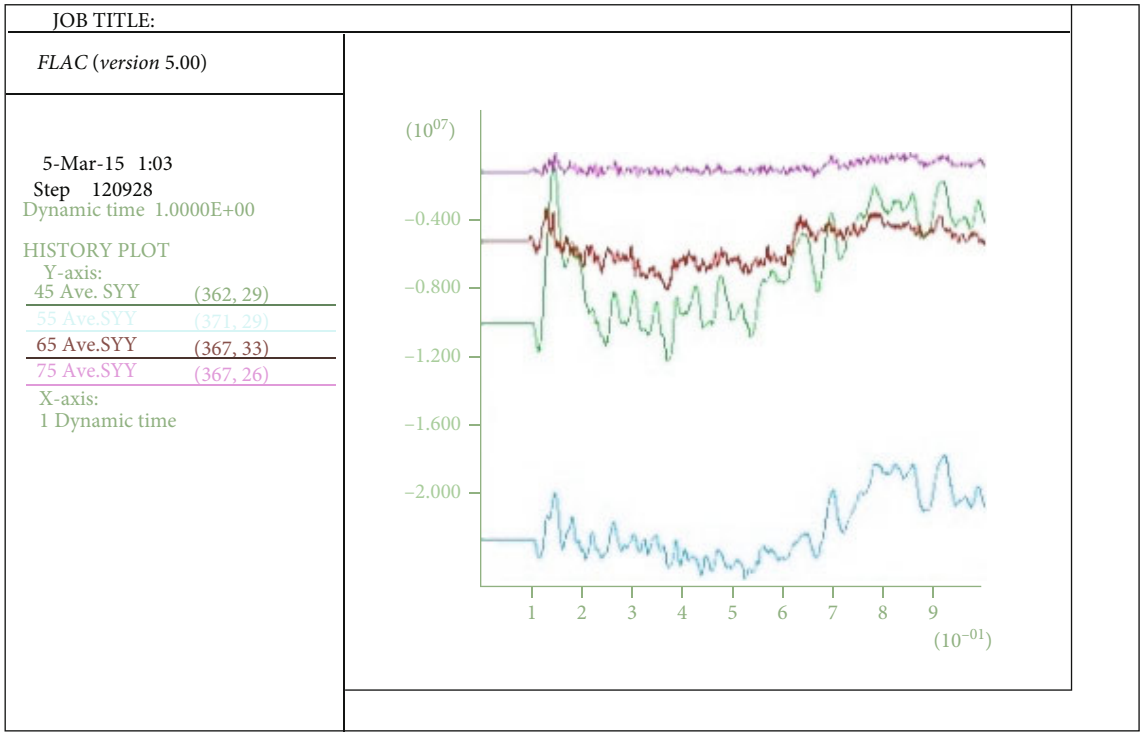

(a) Vertical stress variation of roadway roof, floor, and two sides

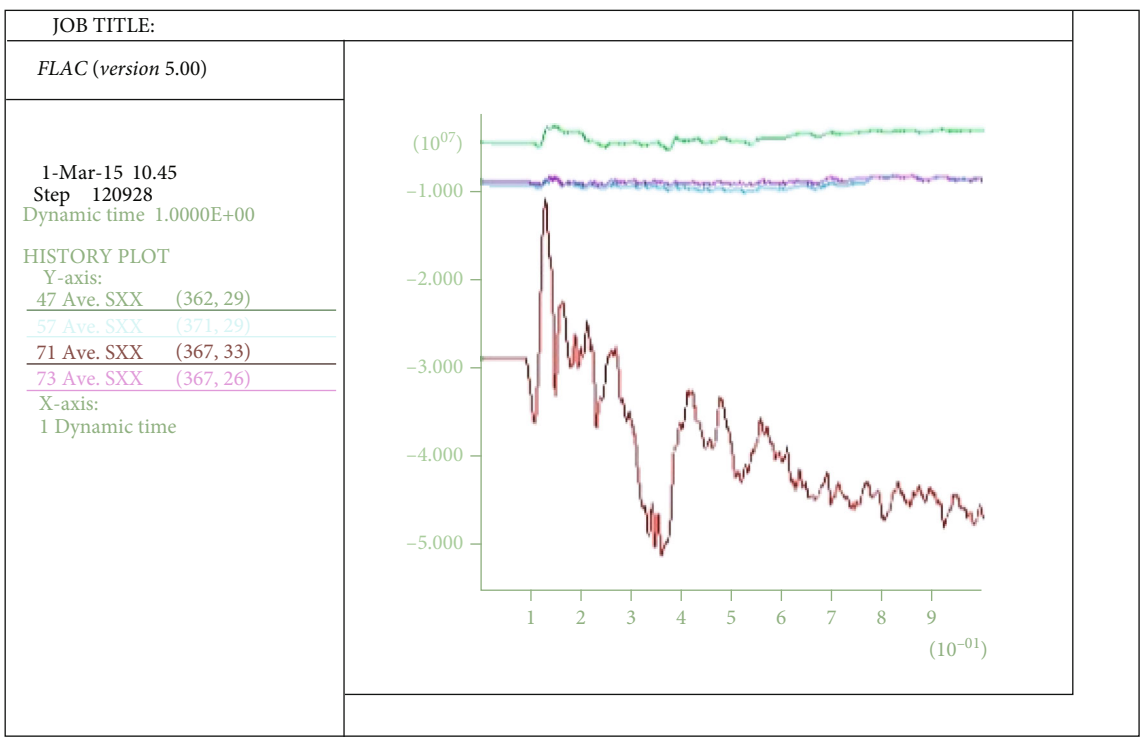

(b) Horizontal stress variation of roadway roof, floor, and two sides

Figure 8: Continued.

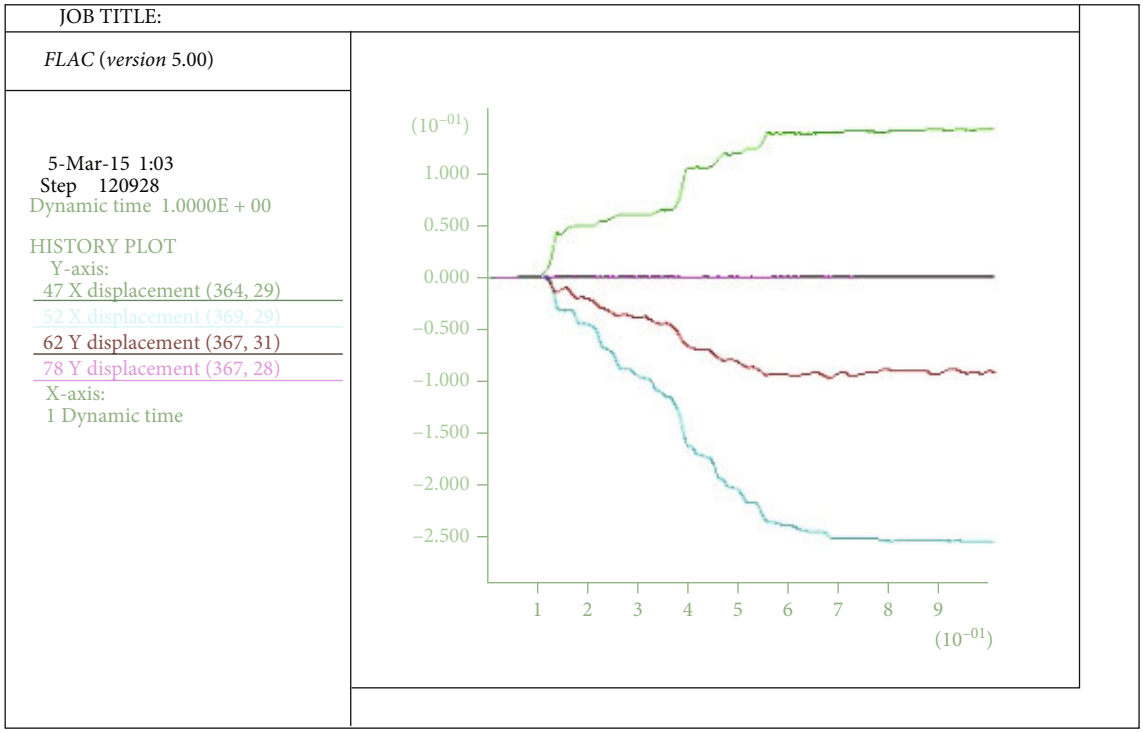

(c) Displacement of roof, floor, and two sides of roadway

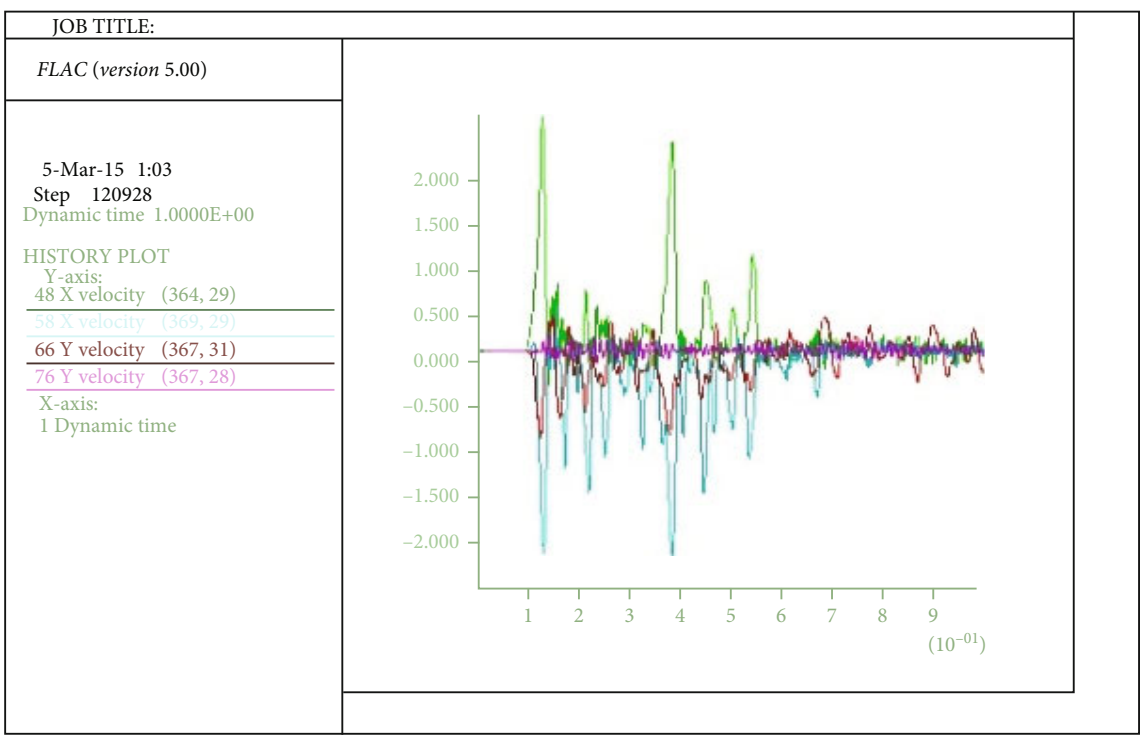

(d) Displacement speed of roadway roof and floor and two sides

Figure 8: Continued.

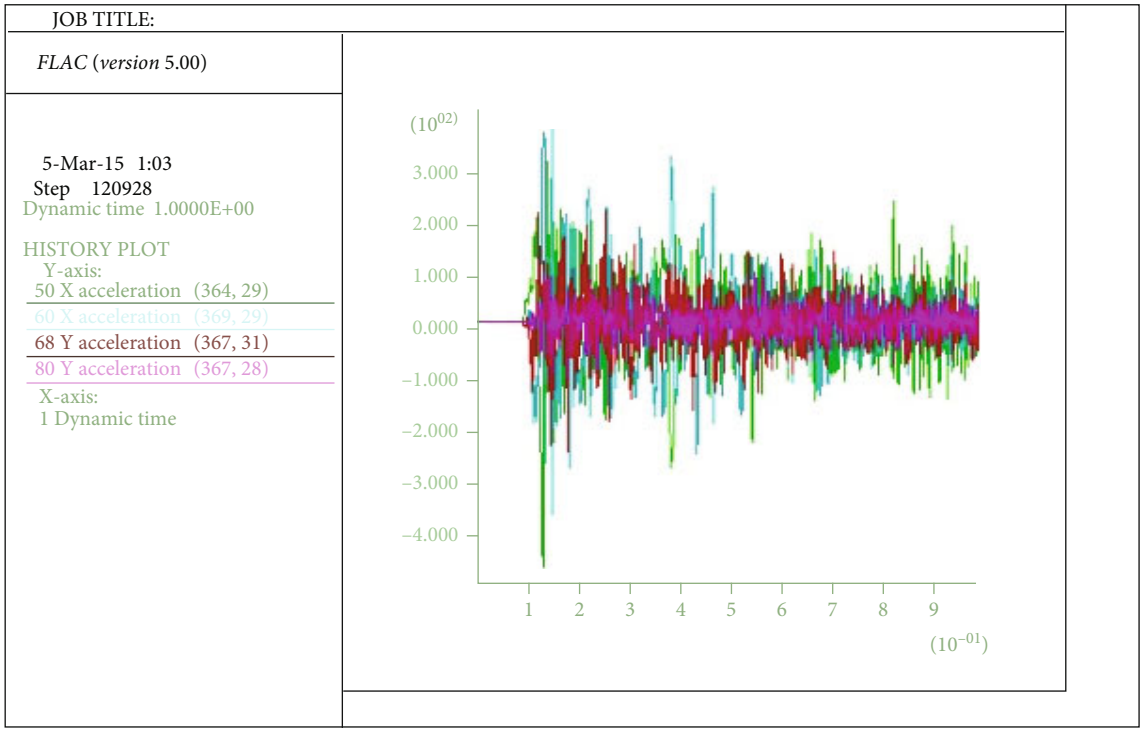

(e) Displacement acceleration of roadway roof and floor and two sides

Figure 8: Dynamic response of surrounding rock of the gob-side roadway.

21.52 MPa. After 0.5 s, the variation range of the stress decreases, and the horizontal stress fluctuates up and down around 9–16 MPa. The horizontal stress state of both sides and floor is less affected by mine earthquake, and the stress basically reaches a stable state after 0.4 s disturbance. The vertical stress of the top and bottom plate is at a low level, which is basically stable after 0.4 s disturbance. The evolution law of approach velocity and acceleration is generally consistent with the solid coal conditions on both sides. The approach of the two sides basically reaches a stable state after 0.6 s disturbance.

It can be seen from Figures 7 and 8 that under the dual influence of lateral abutment pressure and disturbance in goaf, the dynamic response degree of the gob-side roadway is significantly higher than that of solid coal roadway.

In terms of stress, the vertical stress of the outer side (23.2 MPa) is higher than that of the inner side (12.34 MPa), but the change of the vertical stress of the outer side is relatively gentle compared with that of the inner side. In the process of strong earthquake disturbance, the horizontal stress of the roof of the roadway along the goaf has been in a high stress state, and the maximum value has reached 55.28 MPa. The probability of shear failure of the roof has been significantly strengthened. Compared with solid coal roadway, the vertical stress and horizontal stress of the gob-side roadway have been fluctuating, which is difficult to achieve stability.

In terms of displacement, the convergence of surrounding rock of the gob-side roadway is significantly greater than that of solid coal roadway, and the convergence of two sides is more obvious. The stability of the outer upper is poor and the degree of stress concentration is high, resulting in the maximum approach of the outer upper reaches 250.53 mm. The displacement of the inner upper also increased significantly, reaching 139.58 mm. The roof subsidence reached 91.81 mm. Therefore, under the influence of strong earthquake, the risk of side caving, roof separation, or caving of roadway along goaf increases significantly. However, the time required for the displacement of the two sides to reach stability is the same as that of the solid coal roadway, both of which are 0.6 s.

In terms of deformation velocity and acceleration, the deformation velocity and acceleration of the inner side are greater than those of the outer side, and the maximum deformation velocity and deformation acceleration of the inner side reach 2.43 m/s and 469.23 m/s^2, respectively. However, the time when the velocity of the outer side is greater than 1 m/s is significantly higher than that of the inner side, so that the final deformation of the external side is greater than that of the inner side. Compared with the solid coal roadway, the roof displacement of the gob side roadway shows a continuous increasing trend, and the roof does not shock.

According to the dynamic response characteristics of the gob-side roadway and the solid coal roadway, the deformation amount and deformation velocity of the gob-side roadway are greater than those of the solid coal roadway, and the rock burst is more likely to occur in the gob side roadway under the disturbance of strong earthquake. Therefore, it is necessary to predict and judge the breaking and migration of magmatic rock in time during the mining process of the working face and strengthen the support strength of the roadway in the broken area.

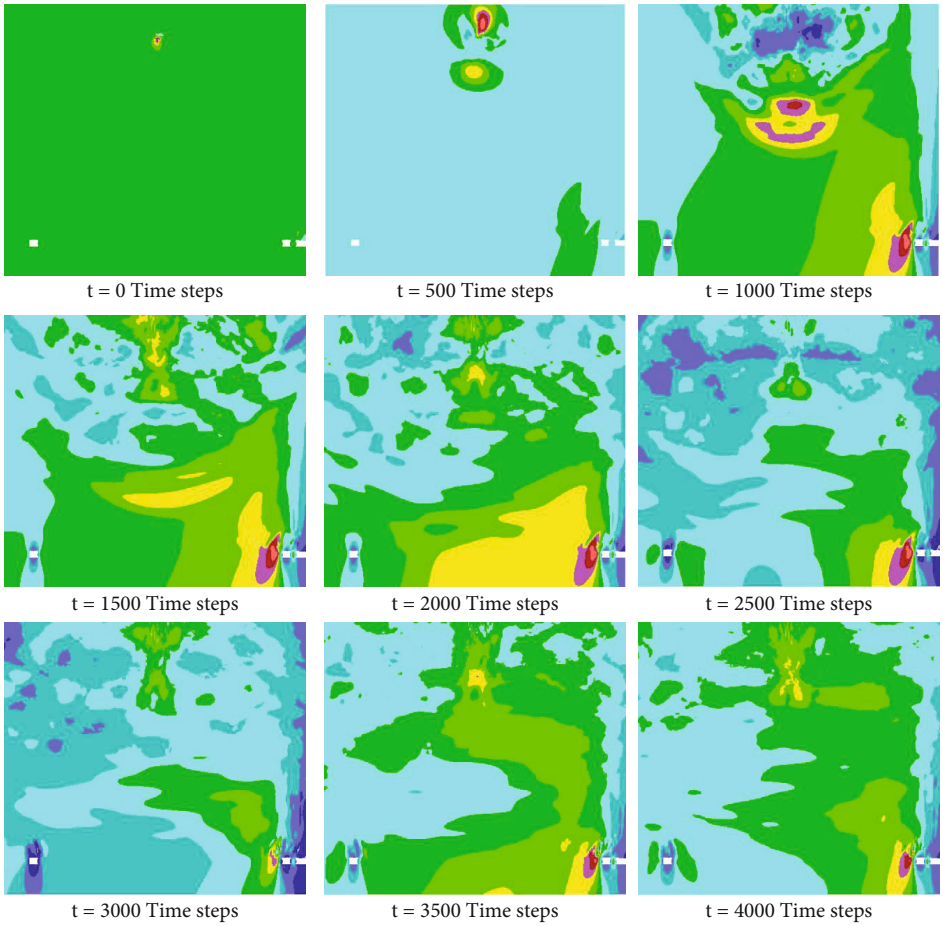

Figure 9: Temporal and spatial evolution law of vertical stress field of roadway surrounding rock under strong earthquake disturbance.

Table 2: Dynamic response of roadway surrounding rock under different boundary conditions.

Boundary condition			Dynamic response				
			Peak value of vertical stress/MPa	Peak value of horizontal stress/MPa	Deformation of surrounding rock/mm	Deformation velocity/m/s	Deformation acceleration/m/s^2
Solid coal face on both sides	Solid coal roadway	Outer side	14.02	4.62	21.05	1.53	404
		Inner side	19.36	7.42	27.28	1.54	366
		Roof	4.89	20.62	10.58	1.33	261
		Floor	2.13	6.25	0.67	0.19	94
One side gob face working face	Solid coal roadway	Outer side	13.76	4.26	18.16	1.32	386.27
		Inner side	19.18	7.06	24.54	1.47	1107.63
		Roof	6.67	21.52	9.63	1.25	236.96
		Floor	2.11	6.33	0.61	0.21	191.03
	Gob-side roadway	Outer side	23.2	8.44	250.53	2.11	369.69
		Inner side	12.34	3.02	139.58	2.43	469.23
		Roof	8.87	55.28	91.81	0.91	248.38
		Floor	3.14	7.83	0.2	0.17	110.65

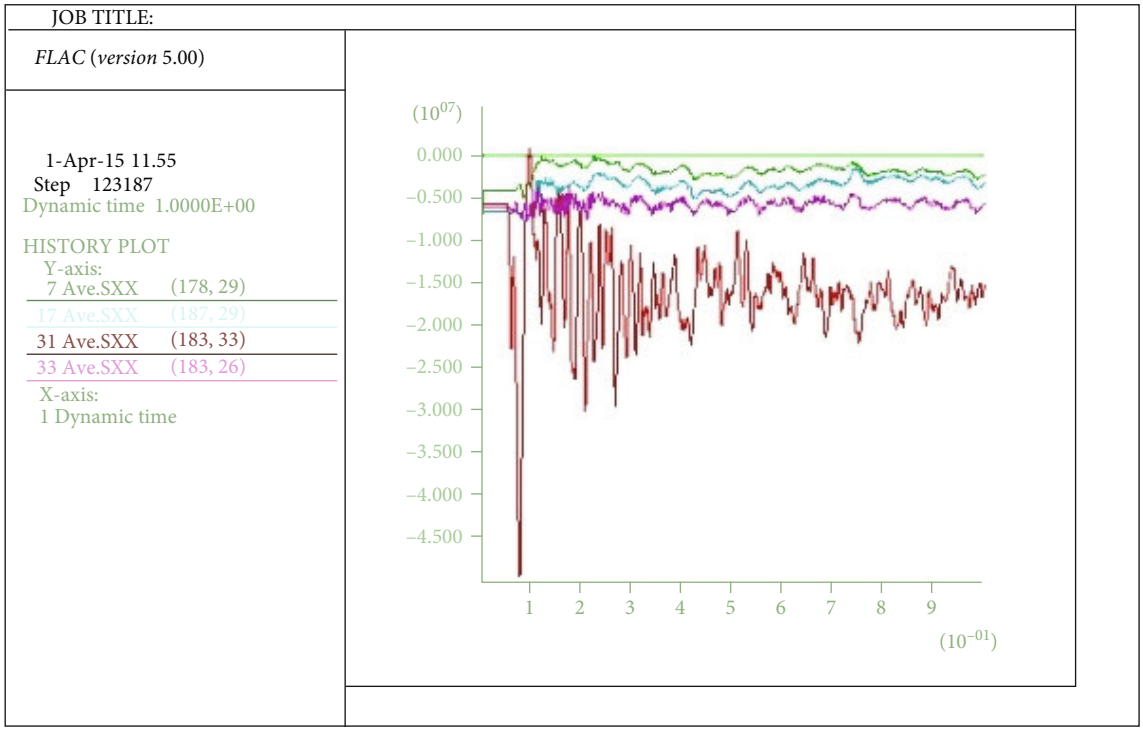

(a) Horizontal variation of roadway floor and roof stress

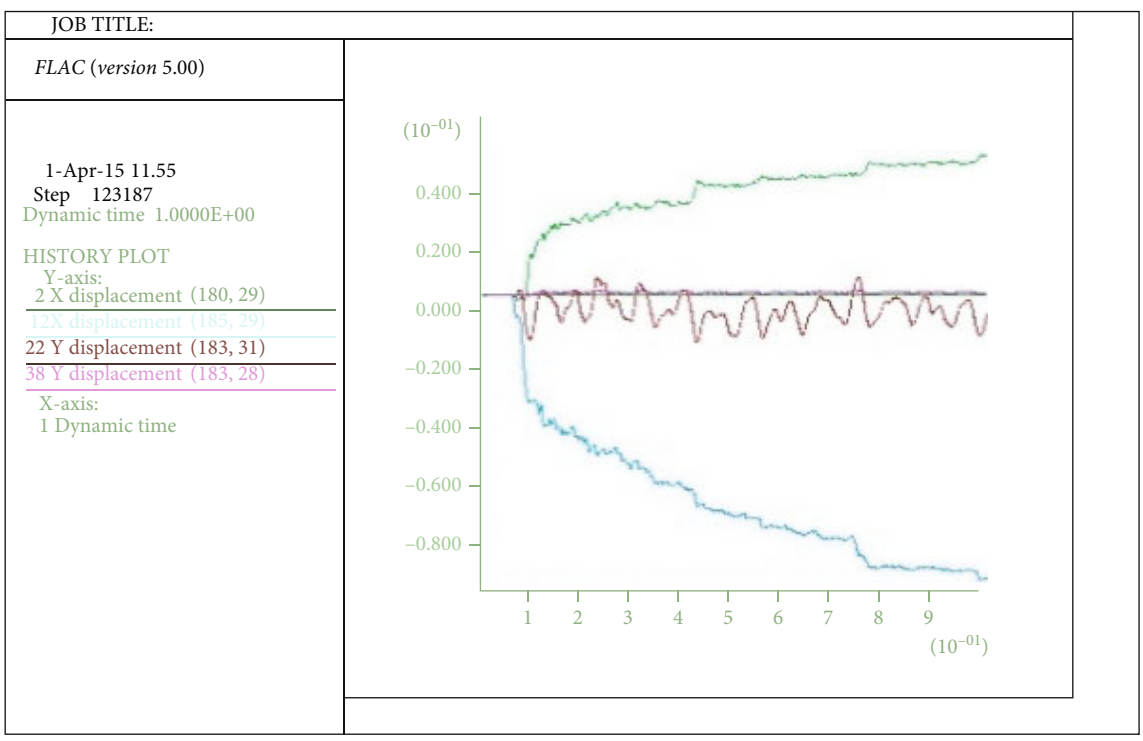

(b) Displacement of roof, floor, and two sides of roadway

Figure 10: Continued.

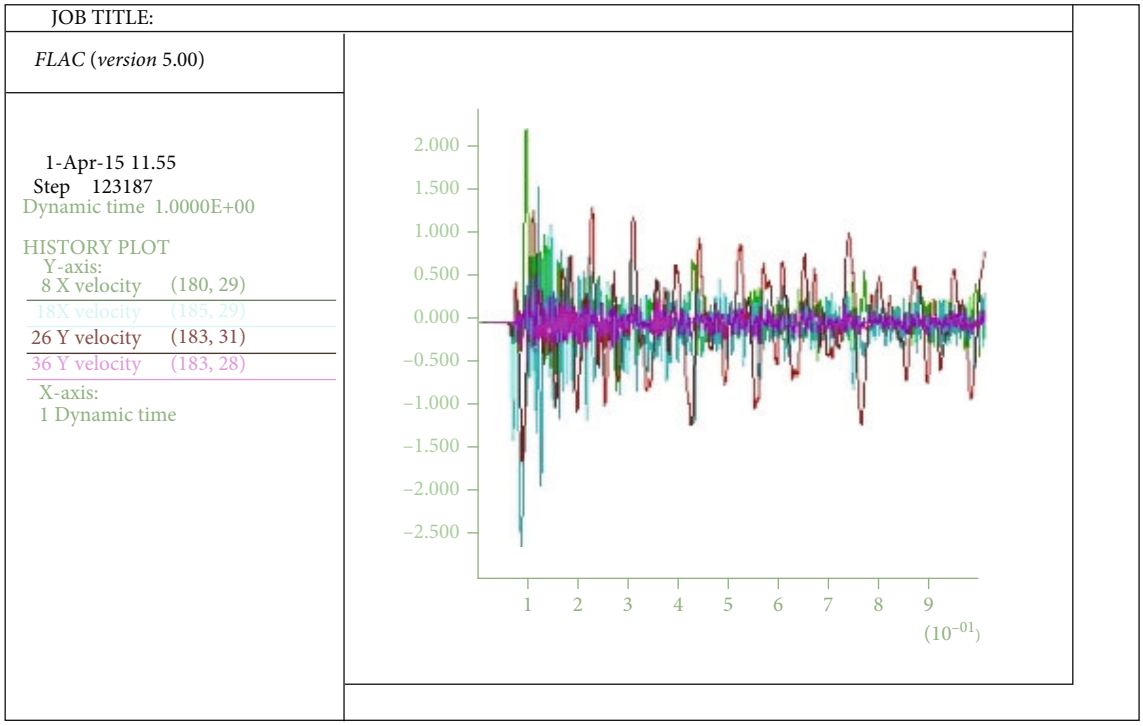

(c) Displacement speed of roadway roof and floor and two sides

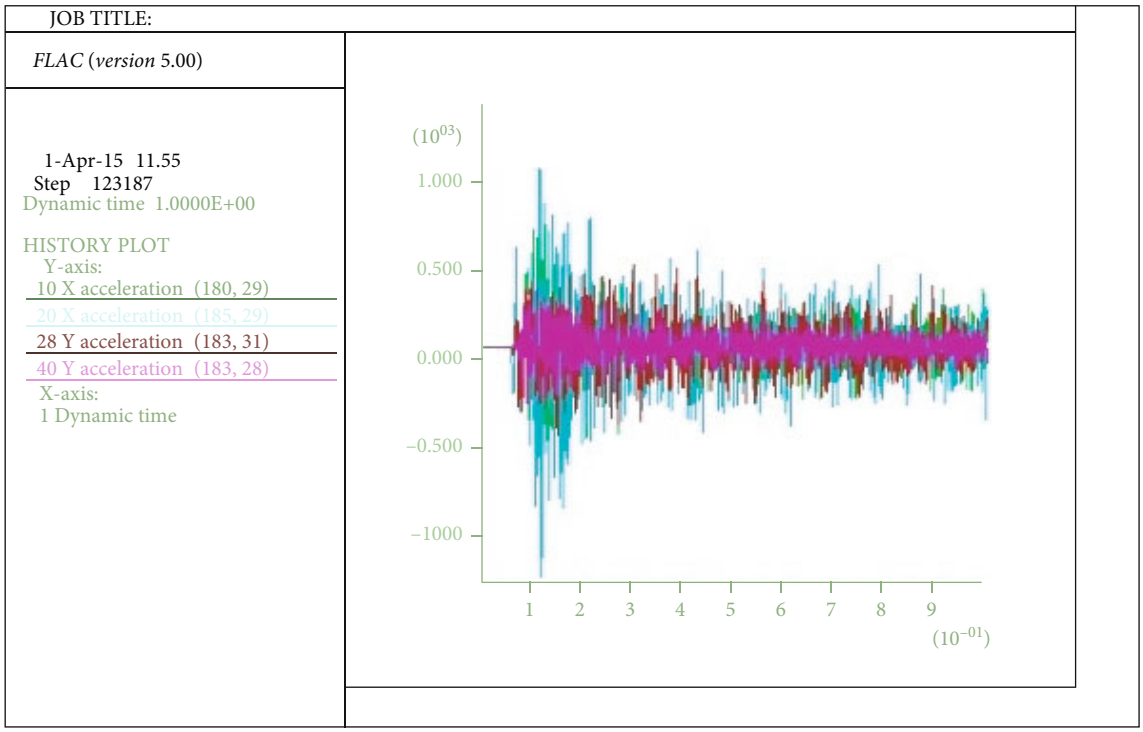

(d) Displacement acceleration of roadway roof and floor and two sides

Figure 10: Dynamic response of surrounding rock of solid coal roadway when the seismic focus height is 50 m.

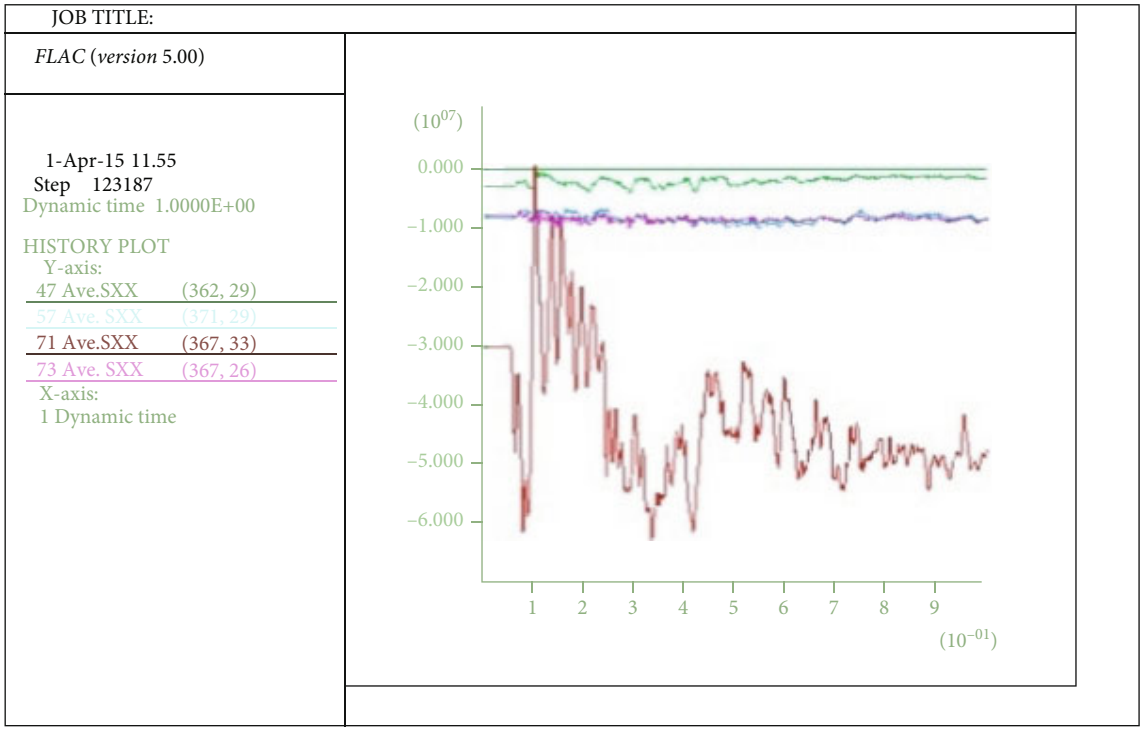

(a) Horizontal variation of roadway floor and roof stress

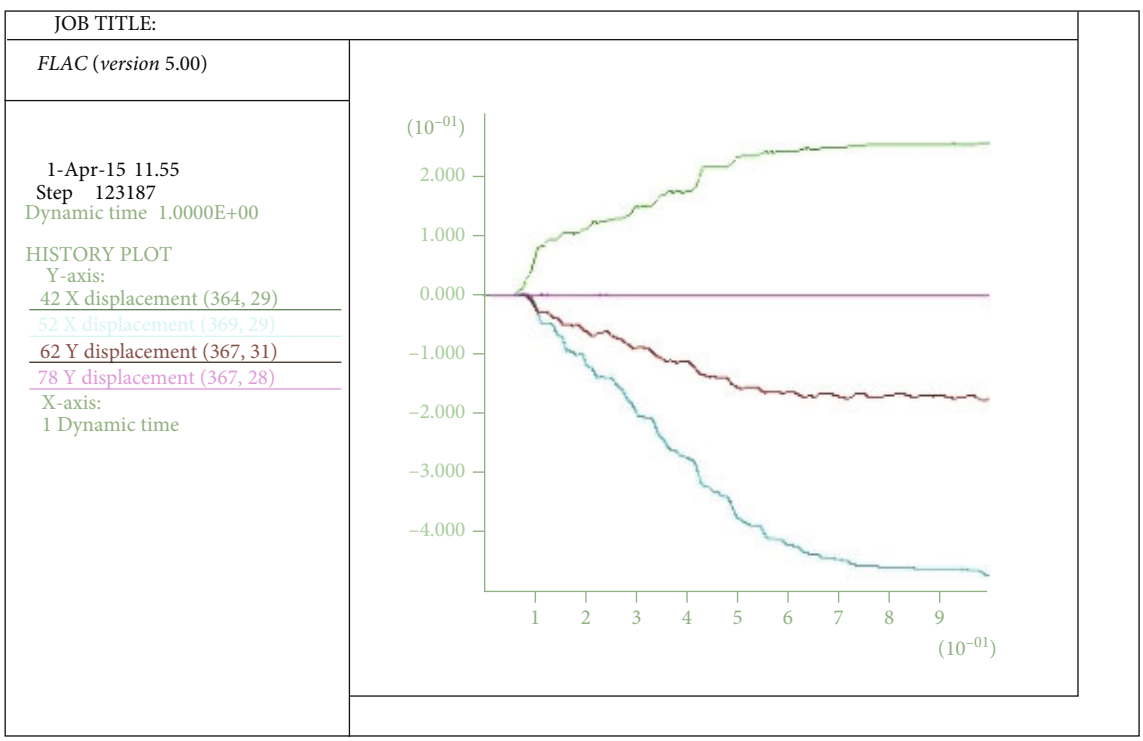

(b) Displacement of roof, floor, and two sides of roadway

Figure 11: Continued.

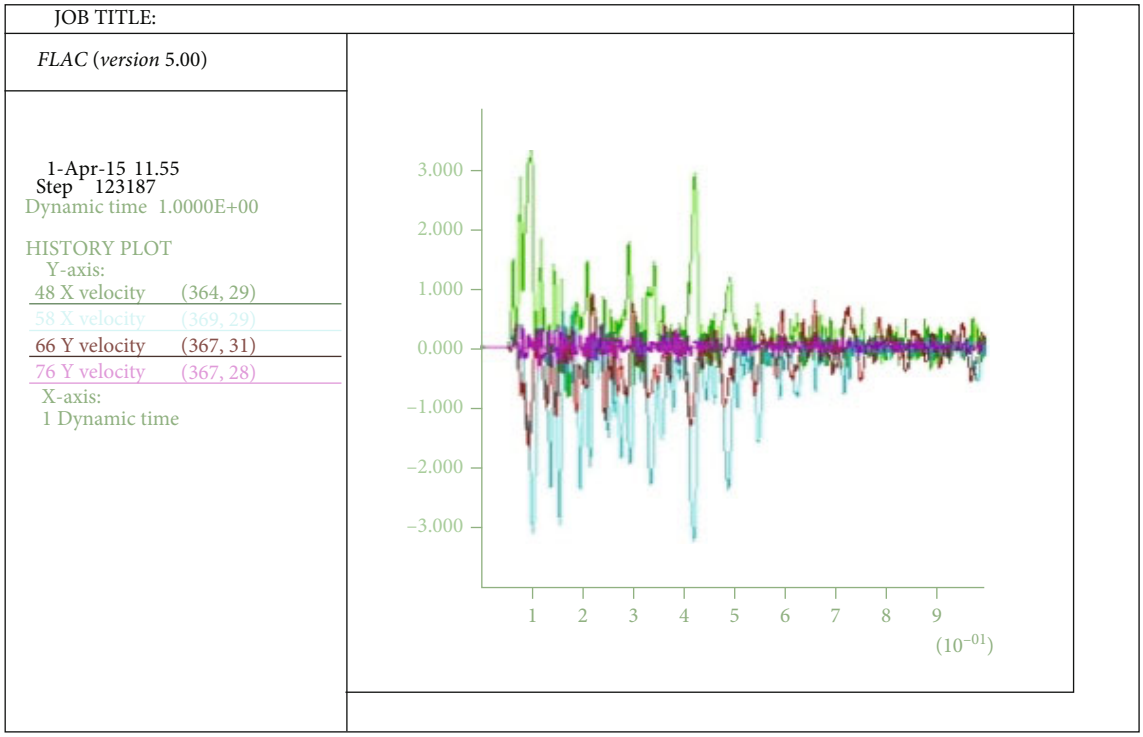

(c) Displacement speed of roadway roof and floor and two sides

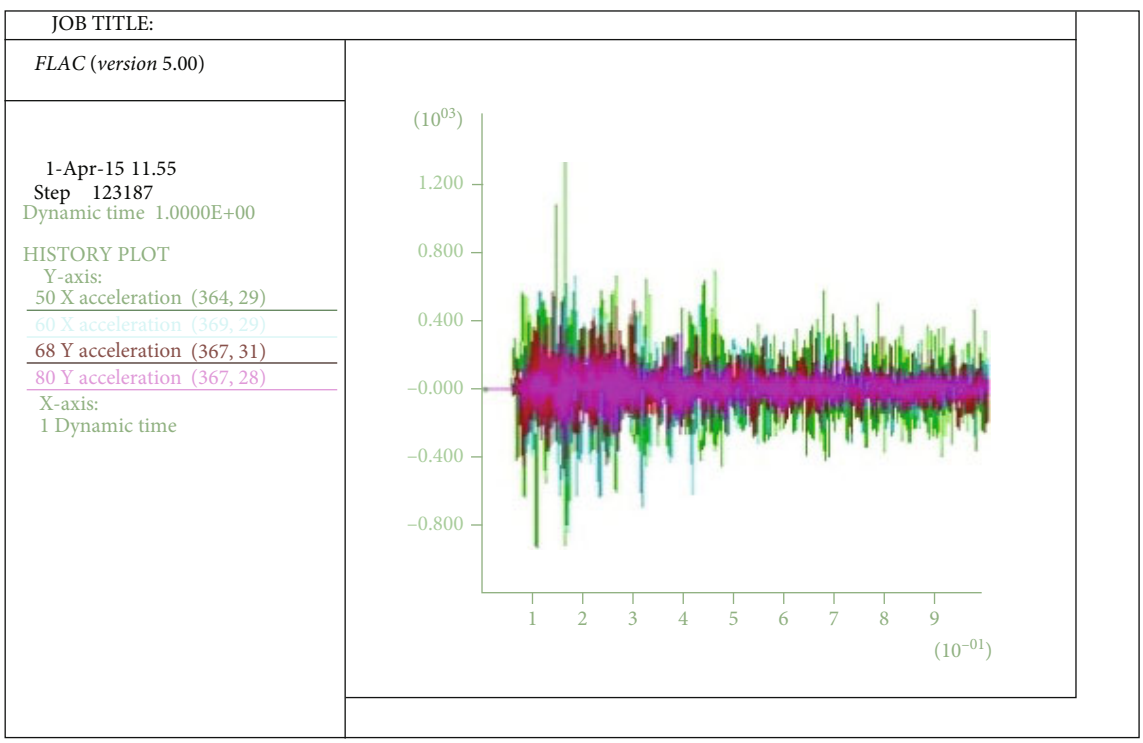

(d) Displacement acceleration of roadway roof and floor and two sides

Figure 11: Dynamic response of surrounding rock of gob roadway when the seismic focus height is 50 m.

Table 3: Dynamic response of surrounding rock of roadway with different seismic focus height under the condition of solid coal on both sides.

Seismic focus height		Dynamic response				
		Peak value of vertical stress/MPa	Peak value of horizontal stress/MPa	Deformation of surrounding rock/mm	Deformation velocity/m/s	Deformation acceleration/m/s^2
113 m	Outer side	14.02	4.62	21.05	1.53	404
	Inner side	19.36	7.42	27.28	1.54	887.07
	Roof	4.89	20.62	10.58	1.33	261
	Floor	2.13	6.25	0.25	0.19	94
90 m	Outer side	13.77	4.49	28.67	1.09	346.02
	Inner side	20.02	7.52	46.24	1.53	760.31
	Roof	8.03	35.95	20.25	0.96	382.94
	Floor	2.51	6.78	0.81	0.27	180.49
70 m	Outer side	13.37	4.32	29.48	0.966	646.18
	Inner side	19.16	7.34	54.91	1.95	783.97
	Roof	7.20	25.2	15.28	1.31	339.99
	Floor	2.48	6.64	0.96	1.01	213.98
50 m	Outer side	14.19	4.88	51.73	2.19	910
	Inner side	19.06	7.44	115.17	2.58	2344.1
	Roof	6.56	44.77	16.1	1.41	601.85
	Floor	3.46	7.82	1.82	0.57	474.55

4. Spatial Evolution Characteristics of Impact Failure of Roadway Caused by Strong Earthquake

Figure 9 reflects the temporal and spatial evolution characteristics of the stress field of roadway surrounding rock under strong earthquake disturbance. It can be seen from Figure 9 that after the source is applied, the stress also diffuses rapidly in a spherical manner, but the attenuation speed of the stress wave is greater than that of the solid coal on both sides under the goaf condition on one side, and the diffusion of the stress wave tends to the goaf side. Under the combined action of the lateral abutment pressure and disturbance in the goaf, and the stability of the surrounding rock on the goaf side is worse than that of the solid coal, the deformation of the roadway along the goaf side increases rapidly, while the solid coal side is relatively slow.

4.1. Comparative Analysis of Dynamic Response of Roadway Surrounding Rock under Different Boundary Conditions under Strong Earthquake Disturbance. The dynamic response characteristics of roadway surrounding rock under different boundary conditions under the same focal conditions are shown in Table 2. It can be seen from Table 2 that for the same source disturbance, the dynamic response of surrounding rock is obviously different under different roadway boundary conditions, and the failure effect increases with the increase of the number of adjacent goafs, especially the horizontal stress of roof and the horizontal displacement of two sides. For the horizontal stress of the roof, the peak value of the horizontal stress of the roof under the conditions of goaf on both sides and goaf on one side is 3.39 and 2.68 times of the horizontal stress of the roof under the conditions of solid coal on both sides, respectively. The shear instability of the roof support is easy to occur. Therefore, for the mine with hard or even extremely thick key layers on the working face, the isolated working face should be avoided. For the displacement of the side wall, the displacement of the roadway along the goaf is significantly greater than that of the solid coal roadway. Therefore, for the roadway along the goaf, the support of the side wall should be strengthened to prevent the instability of the side wall. Under strong earthquake disturbance, the damage effect of solid coal roadway is low, and the risk caused by strong earthquake is controllable.

5. Influence Law of Seismic Focus Height on Roadway Dynamic Response

Magmatic rocks with different heights from the coal seam lead to the change of the seismic focus height of strong earthquakes. In order to study the influence of the seismic focus height on the dynamic response of roadway, strong seismic disturbance was applied at 50 m, 70 m, and 90 m above the coal seam, respectively.

Taking one side as solid coal and the other side as goaf working face, the seismic focus height is 50 m as an example, and the dynamic response law of roadway surrounding rock under strong earthquake disturbance is studied. Figure 10 reflects the dynamic response characteristics of surrounding rock of solid coal roadway under the condition that one side of the working face is mined out when the focal height is 50 m. It can be seen from Figures 7 and 10 that under the same focal intensity and boundary conditions, when the focal height is 50 m, the seismic damage effect is stronger than that when the focal height is 116 m. Take

Table 4: Dynamic response of roadway surrounding rock with different focal height under one side goaf condition.

Seismic focus height			Dynamic response				
			Peak value of vertical stress/MPa	Peak value of horizontal stress/MPa	Deformation of surrounding rock/mm	Deformation velocity/m/s	Deformation acceleration/m/s^2
116 m	Solid coal roadway	Outer side	13.76	4.26	18.16	1.32	386.27
		Inner side	19.18	7.06	24.54	1.47	1107.63
		Roof	6.67	21.52	9.63	1.25	236.96
		Floor	2.11	6.33	0.61	0.21	191.03
	Gob-side roadway	Outer side	23.2	8.44	250.53	2.11	369.69
		Inner side	12.34	3.02	139.58	2.43	469.23
		Roof	8.87	55.28	91.81	0.91	248.38
		Floor	3.14	7.83	0.2	0.17	110.65
90 m	Solid coal roadway	Outer side	13.64	4.43	33.79	0.94	499.36
		Inner side	19.37	7.59	46.61	1.6	1137.5
		Roof	10.97	29.08	20.45	1.3	322.88
		Floor	2.52	6.8	1.12	0.29	234.14
	Gob-side roadway	Outer side	24.04	9.67	283.65	2.26	464.1
		Inner side	12.56	3.84	198.58	2.57	461.93
		Roof	8.75	61.35	130.89	1.09	376.37
		Floor	3.52	9.04	0.6	0.33	253.52
70 m	Solid coal roadway	Outer side	13.57	4.47	28.5	1.1	602.05
		Inner side	19.52	7.58	49.05	2.12	1245.01
		Roof	7.41	44.92	14.05	1.45	333.4
		Floor	2.25	6.89	0.96	0.25	207.75
	Gob-side roadway	Outer side	24.44	9.41	348.63	2.72	543.54
		Inner side	12.19	3.65	187.39	2.11	738.51
		Roof	9.6	62.03	148.54	1.32	437.73
		Floor	3.64	9.19	0.61	0.22	161.47
50 m	Solid coal roadway	Outer side	14.31	4.97	47.37	2.27	768.42
		Inner side	20.06	7.5	96.42	2.63	1466.62
		Roof	6.82	49.01	16.37	1.62	573.02
		Floor	3.29	7.71	1.55	0.56	401.76
	Gob-side roadway	Outer side	24.84	9.91	471.88	3.29	861.36
		Inner side	12.86	4.03	257.16	3.29	1323.45
		Roof	9.13	63.11	176.67	1.73	564.41
		Floor	4.05	10.28	0.92	0.48	407.03

the horizontal stress of roadway surrounding rock and the approach amount of roadway surrounding rock as an example.

The horizontal stress of roadway roof increases greatly, with the maximum value of 49.01 MPa, which is 2.27 times higher than that under the condition of seismic focus height of 116 m. As a result, the spalling failure of roof is almost inevitable, and the mechanical environment of surrounding rock worsens sharply. The maximum displacement of the outer slope and the inner slope reaches 47.37 mm and 96.42 mm, respectively. The displacement of the surrounding rock is significantly enhanced, which is easy to cause support instability and serious slope, and the vibration amplitude of the roof is also strengthened accordingly.

Figure 11 reflects the dynamic response characteristics of surrounding rock of gob-side roadway under the condition of goaf on one side of the working face when the seismic focus height is 50 m. It can be seen from Figure 11 that after the focal height is reduced, the influence of disturbance on the roadway along the goaf is also significantly strengthened. The maximum horizontal stress of roof reaches 63.11 MPa, and the horizontal stress during disturbance is basically above 33 MPa. The movement of roof, floor, and two sides is also at a high level. The maximum movement of roof is 176 mm, the movement of inner side is 256.41 mm, and the movement of outer side is 471.88 mm, which is 1.9 times of the movement of outer side along the roadway when the seismic focus height is 116 m.

To sum up, when the focal height is 50 m, the vibration effect of gob-side roadway is more intense, and the gob-side roadway becomes the key prevention area of rock burst during the breaking and migration of hard and thick key

layer. The support strength of roof and two sides should be increased to reduce the risk of impact.

In order to better reflect the influence of seismic focus height on roadway dynamic response, the variation characteristics of roadway surrounding rock dynamic response at different focal height are counted, as shown in Tables 3 and 4. It can be seen from Tables 3 and 4 that under the condition of the same seismic focus intensity, when the focal point is 116 m above the coal seam, the vibration effect of roadway surrounding rock is relatively small. As the focal height decreases, the damage degree of roadway surrounding rock increases and the stability of surrounding rock becomes worse.

Taking one side gob condition as an example, the influence of seismic focus height on the stability of roadway surrounding rock is analyzed. It can be seen from Table 4 that with the continuous decrease of seismic focus height, the disturbance effect of strong earthquake on roadway continues to strengthen, but there is a significant difference in strengthening rate. When the focal height decreases from 116 m to 90 m, the horizontal stress of the roof, the displacement of the side and roof, the approaching velocity, and the approaching acceleration begin to increase, but the increment is small. When the seismic focus height decreases from 90 m to 50 m, the increment increases rapidly in a nearly linear manner. Taking the horizontal approach of the outer wall of the roadway along the goaf as an example, when the seismic focus height is reduced from 116 m to 90 m, the approach increases by only 33.12 mm, while when the seismic focus height is reduced from 90 m to 50 m, the approach increases by 188.23 mm. In addition, with different roadway boundary conditions, the influence degree of focal height on roadway is also different. The influence degree of horizontal stress of solid coal roadway roof is much greater than that of goaf roadway. Regardless of the boundary conditions, the vertical stress of the roadway slope is less affected by the focal height.

To sum up, when a strong earthquake occurs in the lower position, the dynamic response degree of the roadway is much greater than that in the higher position, and the influence degree of the goaf side is greater than that of the solid coal side. In addition, when the seismic focus height is the same, the influence degree of strong earthquake on the stability of roadway surrounding rock under different boundary conditions is also significantly different. Basically, the influence degree can be arranged as follows: gob-side roadway (mined out on one side) > solid coal roadway (mined out on both sides) > solid coal roadway (mined out on one side). The strong earthquake tends to the goaf side in the transmission process, resulting in the energy of solid coal roadway under the goaf condition on one side is lower than that under the solid condition on both sides, and resulting in the dynamic response of solid coal roadway under the goaf condition on one side is weaker than that under the solid coal condition on both sides. Combined with the roadway stress level before dynamic load disturbance, under the condition of high static load, the stability of roadway surrounding rock is more obviously affected by dynamic load. The greater the static load level is, the worse the stability of surrounding rock is, that is, the higher the static load level is, the more obvious the coupling effect with dynamic load is.

6. Conclusion

Using the dynamic calculation function of FLAC2D software, this paper analyzes the dynamic response of roadway surrounding rock under strong earthquake disturbance when it is covered with hard and thick key layer, studies the influence of roadway boundary conditions on the dynamic response of surrounding rock under strong earthquake disturbance and the effect of the seismic focus height on the impact damage degree of roadway, and simulates and reproduces the dynamic evolution process of roadway degeneration damage. The main conclusions are as follows:

(1) Under the influence of strong earthquake, the stress level of gob-side roadway is higher than that of solid coal roadway, especially the horizontal stress of roof, which is easy to lead to the instability of roof support. The stress level of the outer side of the gob-side roadway is higher than that of the inner side. The gob coal pillar is in a high stress state, and the coal pillar is easy to lose stability

(2) Under the influence of strong earthquake, the roof of solid coal roadway is easy to vibrate in a small range, and the displacement increases and decreases with the disturbance. The displacement of the floor and two sides of the solid coal roadway and the top floor and two sides of the roadway along the goaf continues to increase in the initial stage of the disturbance, and the displacement will remain stable with the continuation of the disturbance. The displacement of both sides and roof and floor of gob-side roadway can reach stability in the later stage of disturbance, and with the increase of the number of adjacent goaf, the longer it takes for the displacement of surrounding rock to reach stability

(3) There is a close correlation between the seismic focus height and the dynamic response of roadway surrounding rock. The magnitude of stress field, displacement field, velocity field, and acceleration field of roadway surrounding rock is negatively correlated with the seismic focus height. When the seismic focus height is lower than 90 m, the variation of surrounding rock response increases sharply with the decrease of the seismic focus height. When a strong earthquake occurs in the low rock stratum, the impact damage of roadway surrounding rock is almost inevitable

(4) The influence degree of strong earthquake on the stability of roadway surrounding rock is arranged as follows: gob-side roadway (mined out on one side) > solid coal roadway (mined out on both sides) > solid coal roadway (mined out on one side). According to the dynamic response degree of surrounding rock under different boundary conditions, the greater the static load level

before strong earthquake disturbance, the more obvious the coupling effect with dynamic load

(5) The spatial evolution of roadway impact failure caused by strong earthquake shows that the working face boundary conditions have an important influence on the energy propagation of mine earthquake. When there is solid coal on both sides of the working face, the energy basically propagates to the two lanes of the working face in a symmetrical way. When one side of the working face is mined out, the energy transfer is biased to the side of the goaf. The evolution process also shows that with the increase of the number of adjacent goafs, the faster the attenuation rate of mine earthquake propagation energy

Data Availability

The data used to support the findings of this study are included within the article.

Conflicts of Interest

The authors declare that there are no conflicts of interest related to the publication of this paper.

Acknowledgments

This research was funded by the Natural Foundation of Shandong Province (Grant no. ZR2020QE121), the Postdoctoral Innovation Project of Shandong Province (Grant no. 202003090), the Postdoctoral Science Foundation of China (Grant no. 2020M682267), Engineering Laboratory of Deep Mine Rockburst Disaster Assessment Open Project (LMYK002), and the Jining key research and development plan (Grant no. 2020JNZC002).

References

[1] D. Chlebowski, A. Zorychta, Z. Burtan, and M. Cała, "Location of opening-out cross-cuts in relation to rockburst hazard conditions along the face in the light of model testing," *Archives of Mining Sciences*, vol. 62, no. 1, pp. 121–130, 2017.

[2] L. S. Jiang, P. P. Zhang, L. J. Chen et al., "Numerical approach for goaf-side entry layout and yield pillar design in fractured ground conditions," *Rock Mechanics and Rock Engineering*, vol. 50, no. 11, pp. 3049–3071, 2017.

[3] Y. Y. Wen, Z. L. Mu, E. B. Yi, H. Wang, and Z. J. Liu, "The response features of roadway surrounding rock in different hardness coal seams under dynamic disturbance," *Journal of Mining and Safety Engineering*, vol. 30, no. 4, pp. 555–559, 2013.

[4] A. Sainoki and H. S. Mitri, "Simulating intense shock pulses due to asperities during fault-slip," *Journal of Applied Geophysics*, vol. 103, pp. 71–81, 2014.

[5] G. Mutke, J. Dubiński, and A. Lurka, "New criteria to assess seismic and rock burst hazard in coal mines / nowe kryteria dla oceny zagrożenia sejsmicznego I tąpaniami W kopalniach węgla kamiennego," *Archives of Mining Sciences*, vol. 60, no. 3, pp. 743–760, 2015.

[6] A. Mortazavi and F. T. Alavi, "A numerical study of the behavior of fully grouted rockbolts under dynamic loading," *Soil Dynamics and Earthquake Engineering*, vol. 54, pp. 66–72, 2013.

[7] C. P. Lu, Y. Liu, H. Y. Wang, and P. F. Liu, "Microseismic signals of double-layer hard and thick igneous strata separation and fracturing," *International Journal of Coal Geology*, vol. 160-161, pp. 28–41, 2016.

[8] L. Wang, Y. P. Cheng, C. Xu, F. H. An, K. Jin, and X. L. Zhang, "The controlling effect of thick-hard igneous rock on pressure relief gas drainage and dynamic disasters in outburst coal seams," *Natural Hazards*, vol. 66, no. 2, pp. 1221–1241, 2013.

[9] W. J. Guo, Y. Y. Li, D. W. Yin, S. C. Zhang, and X. Z. Sun, "Mechanisms of rock burst in hard and thick upper strata and rock-burst controlling technology," *Arabian Journal of Geosciences*, vol. 9, no. 10, p. 561, 2016.

[10] Q. S. Wu, L. S. Jiang, Q. L. Wu, Y. C. Xue, and G. Bing, "A study on the law of overlying strata migration and separation space evolution under hard and thick strata in underground coal mining by similar simulation," *DYNA-Ingeniería e Industria*, vol. 93, no. 1, pp. 175–181, 2018.

[11] J. L. S. Jiang, Q. S. Wu, Q. L. Wu, P. Wang, Y. C. Xue, and G. Bing, "Fracture failure analysis of hard and thick key layer and its dynamic response characteristics," *Engineering Failure Analysis*, vol. 98, pp. 118–130, 2019.

[12] A. Y. Cao, L. L. Zhu, F. C. Li, L. M. Dou, Y. L. Zhao, and Z. L. Zhang, "Characteristics of T-type overburden structure and tremor activity in isolated face mining under thick-hard strata," *Journal China Coal Sciences*, vol. 39, no. 2, pp. 328–335, 2014.

[13] W. Wang, Y. P. Cheng, H. F. Wang, W. Li, and L. Wang, "Coupled disaster-causing mechanisms of strata pressure behavior and abnormal gas emissions in underground coal extraction," *Environment and Earth Science*, vol. 74, no. 9, pp. 1–9, 2015.

[14] W. Wang, Y. P. Cheng, H. F. Wang et al., "Fracture failure analysis of hard-thick sandstone roof and its controlling effect on gas emission in underground ultra-thick coal extraction," *Engineering Failure Analysis*, vol. 54, pp. 150–162, 2015.

[15] J. Wang, J. G. Ning, and J. Q. Jiang, "Research on the energy criterion for rockbursts induced by broken hard and thick rock strata and its application," *Geotechnical & Geological Engineering*, vol. 35, no. 2, pp. 1–16, 2016.

[16] F. Ju, M. Xiao, Z. He, P. Ning, and P. Huang, "Study on fracture and stress evolution characteristics of ultra-thick hard sandstone roof in the fully mechanized mining face with large mining height: a case study of Xiaojihan coal mine in western China," *Engineering*, vol. 10, pp. 1–12, 2018.

[17] J. L. Xu and M. G. Qian, "Method to distinguish key strata in overburden," *Journal of China University of Mining and Technology*, vol. 29, pp. 463–467, 2000.

[18] S. Zhou, K. Wu, D. Zhou, L. Li, and Y. Xu, "Experimental study on displacement field of strata overlying goaf with sloping coal seam," *Geotechnical and Geological Engineering*, vol. 34, no. 6, pp. 1–10, 2016.

[19] J. L. Xu, M. G. Qian, and W. B. Zhu, "Study on influences of primary key stratum on surface dynamic subsidence," *Chinese Journal of Rock Mechanics and Engineering*, vol. 24, no. 5, pp. 787–791, 2005.

[20] Q. S. Wu, Q. L. Wu, Y. C. Xue, and G. Bing, "Analysis of overlying strata movement and disaster-causing effects of coal

mining face under the action of hard thick magmatic rock," *Processes*, vol. 6, no. 9, p. 150, 2018.

[21] H. He, L. M. Dou, and S. Y. He, "Rock burst rules induced by cracking of overlying key stratum," *Chinese Journal of Geotechnical Engineering*, vol. 32, no. 8, pp. 1221–1241, 2010.

[22] M. J. Hu, L. G. Wang, S. S. Zhu, X. Sun, and G. Zhang, "Reasons and prevention measures for rock burst caused by extremely thick igneous rock," *Mining Research and Development*, vol. 33, pp. 54–57, 2013.

[23] J. Q. Jiang, Q. S. Wu, Q. L. Wu, W. Pu, and B. Gong, "Study on distribution characteristics of mining stress and elastic energy under hard and thick igneous rocks," *Geotechnical and Geological Engineering*, vol. 2, pp. 3451–3466, 2018.

[24] Q. S. Wu, J. Q. Jiang, Q. L. Wu, Y. C. Xue, and B. Gong, "Study on the fracture of hard and thick sandstone and the distribution characteristics of microseismic activity," *Geotechnical and Geological Engineering*, vol. 1, pp. 1–17, 2018.

[25] J. G. Ning, J. Wang, L. S. Jiang, X. S. Liu, and J. Q. Jiang, "Fracture analysis of double-layer hard and thick roof and the controlling effect on strata behavior: a case study," *Engineering Failure Analysis*, vol. 81, pp. 117–134, 2017.

[26] P. J. Yang, Y. He, and W. B. Guo, "Disaster-causing mechanism and control measures of extremely thick and hard magmatic rock above working face," *Journal of China Coal Society*, vol. 38, no. 12, pp. 2106–2112, 2013.